MARTIN MARIETTA ENERGY SYSTEMS LIBRARIES

3 4456 0364226 2

ORNL-3052
UC-4 - Chemistry-General

A PARAMAGNETIC RESONANCE STUDY OF HYPERFINE INTERACTIONS IN SINGLE CRYSTALS CONTAINING α,α-DIPHENYL-β-PICRYLHYDRAZYL

R. W. Holmberg

OAK RIDGE NATIONAL LABORATORY
operated by
UNION CARBIDE CORPORATION
for the
U.S. ATOMIC ENERGY COMMISSION

LEGAL NOTICE

This report was prepared as an account of Government sponsored work. Neither the United States, nor the Commission, nor any person acting on behalf of the Commission:

A. Makes any warranty or representation, expressed or implied, with respect to the accuracy, completeness, or usefulness of the information contained in this report, or that the use of any information, apparatus, method, or process disclosed in this report may not infringe privately owned rights; or

B. Assumes any liabilities with respect to the use of, or for damages resulting from the use of any information, apparatus, method, or process disclosed in this report.

As used in the above, "person acting on behalf of the Commission" includes any employee or contractor of the Commission, or employee of such contractor, to the extent that such employee or contractor of the Commission, or employee of such contractor prepares, disseminates, or provides access to, any information pursuant to his employment or contract with the Commission, or his employment with such contractor.

ORNL-3052

Contract No. W-7405-eng-26

CHEMISTRY DIVISION

A PARAMAGNETIC RESONANCE STUDY OF HYPERFINE INTERACTIONS IN SINGLE CRYSTALS CONTAINING α,α-DIPHENYL-β-PICRYLHYDRAZYL

R. W. Holmberg

Submitted as a thesis to the Graduate Council of The University of Tennessee in partial fulfillment of the requirements for the Degree of Doctor of Philosophy

DATE ISSUED

JAN 24 1961

OAK RIDGE NATIONAL LABORATORY
Oak Ridge, Tennessee
operated by
UNION CARBIDE CORPORATION
for the
U.S. ATOMIC ENERGY COMMISSION

MARTIN MARIETTA ENERGY SYSTEMS LIBRARIES

3 4456 0364226 2

ACKNOWLEDGMENT

The author wishes to express his gratitude to Dr. Ralph Livingston, Professor William T. Smith, Jr., and Dr. Henry Zeldes for their encouragement and helpful cooperation during the course of this research. Thanks are also due to Mr. R. D. Ellison for x-ray examinations, to Dr. W. R. Busing for computer programming, and to Miss Joanne Davenport for secretarial services.

This research was carried out at the Oak Ridge National Laboratory operated for the Atomic Energy Commission by Union Carbide Nuclear Company.

TABLE OF CONTENTS

CHAPTER		PAGE
I.	INTRODUCTION	1
	A. Basic Principles of Paramagnetic Resonance	1
	B. Previous Work on DPPH	13
II.	EXPERIMENTAL	19
	A. Preparation of Materials	19
	B. Growth and Properties of Crystals	21
	C. Spectrometer	26
III.	EXPERIMENTAL RESULTS	33
	A. Theory	33
	B. General Features of Spectra	38
	C. Evaluation of Hyperfine Tensors	44
IV.	INTERPRETATION AND DISCUSSION	60
BIBLIOGRAPHY		75

LIST OF FIGURES

FIGURE PAGE

1. Energy Levels and Hyperfine Spectrum for an Unpaired Electron (S = 1/2) Interacting with a Nucleus of Spin I = 3/2 7
2. Hyperfine Splittings from Two Nitrogen Nuclei in DPPH 8
3. Paramagnetic Resonance Spectra from Dilute DPPH Solutions . . 17
4. Schematic Diagram of a Paramagnetic Resonance Spectrometer. . 27
5. Spectra of a Single Crystal Containing N^{15} Labelled DPPH. The Magnetic Field was Parallel to the AC Plane 40
6. Spectra of a Single Crystal Containing Normal DPPH. The Magnetic Field was Parallel to the AC Plane 41
7. Spectra of a Single Crystal Containing N^{15} Labelled DPPH. The Magnetic Field was Parallel to the AB Plane 42
8. Spectra of a Single Crystal Containing N^{15} Labelled DPPH. The Magnetic Field was Parallel to the BC Plane 43
9. Measured Values and Calculated Curves for the Hyperfine Separations in a Crystal Containing N^{15} Labelled DPPH. The Magnetic Field was Parallel to the AC Plane 48
10. Measured Values and Calculated Curves for the Overall Hyperfine Separation in a Single Crystal Containing N^{15} Labelled DPPH. The Magnetic Field was Parallel to the AB Plane. . . . 49

11. Measured Values and Calculated Curves for the Overall Hyperfine Separation in a Single Crystal Containing N^{15} Labelled DPPH. The Magnetic Field was Parallel to the BC Plane 50

12. Measured Values and Calculated Curves for the Hyperfine Separations in a $DPPH_2$ Crystal Containing Normal DPPH. The Magnetic Field was Parallel to the AC Plane 52

13. Axis System Used in Evaluating Hyperfine Tensors 53

14. Schematic Diagram of Six Line Hyperfine Spectrum Defining ΔH_α, ΔH_β, and ΔH_t. 54

CHAPTER I

INTRODUCTION

A. Basic Principles of Paramagnetic Resonance

In this section, some of the principles of paramagnetic resonance (electron spin resonance) will be outlined with particular reference to the study of free radicals. The effect was first observed by Zavoisky[1] in 1945 and has since been extensively developed and applied to a variety of fields. Many excellent reviews cover the various ramifications of the subject. Particularly noteworthy are several reviews from the Clarendon Laboratory,[2-5] which treat the method and its application to the study of crystals containing transition ions (both the d and f electron series) and paramagnetic centers produced by irradiation of crystals. A review by Wertz[6] and a book by Ingram[7] consider applications to the study of free radicals.

The discussion in this section will be largely qualitative, and is intended as a background to the investigation reported in this thesis. It will be restricted to those paramagnetic atoms or molecules which have only one unpaired electron; most free radicals fall into this category. Such systems possess magnetic dipole moments resulting from both the orbital motion and the intrinsic spin of the electron. The principles of the method can best be introduced, however, by considering a molecule whose unpaired electron has only spin. This condition is closely approximated by a wide variety of paramagnetic substances. This spin dipole will

interact with an applied magnetic field and, according to quantum mechanical principles, will assume one of two energy states; in one state the electron spin is said to be "parallel" to the field, in the other state "antiparallel". The difference in energy of the states is given by $\Delta E = g\beta H$, where g, the spectroscopic splitting factor, is 2.0023 for a "spin only" electron, β is the Bohr magneton, and H is the strength of the applied field. If the system is subjected to electromagnetic radiation of frequency ν such that

$$h\nu = g\beta H, \tag{1}$$

transitions are induced between the two states, and absorption of electromagnetic energy occurs. A typical paramagnetic resonance spectrometer operating at a microwave frequency of 9000 megacycles requires for g = 2.0023 a magnetic field of ca. 3200 gauss to achieve the resonance condition of Equation 1.

At thermal equilibrium, the two spin states in a substance are populated in accordance with the Boltzman distribution; the ratio of these populations is given by $e^{-g\beta H/kT}$. At room temperature, for fields of 3200 gauss and for g = 2.0023, this factor is 0.9985. Transitions induced by microwave energy from the low to high energy state (absorptive transitions) have the same a priori probability as transitions from the high to low energy state (induced emission). Because of the higher population of spins in the lower energy state, slightly more absorptive transitions occur and there results a net absorption of microwave energy. As energy is absorbed there is a tendency to disturb the equilibrium distribution of states. The populations in the two states tend to equalize.

Thermal equilibrium is re-established by non-radiative interactions of the spins with lattice vibrations. The rate of this process is characterized by a thermal spin-lattice relaxation time. Often, this relaxation time is sufficiently long that, in the presence of high microwave power levels, the surplus population in the lower state is reduced and the amount of absorption decreases. This effect is called power saturation.

While paramagnetic resonance can be observed at any frequency, provided the magnetic field is adjusted to fulfill the resonance condition of Equation 1, most spectrometers operate in the microwave region. The so-called x-band spectrometer, operating at 9000 Mc (fields of 3200 gauss for $g = 2$) is widely used for free radical studies. High sensitivity is obtained at these high frequencies and fields. Transition probabilities are larger at high frequencies, and there is a more favorable ratio of spin populations at high fields as indicated by the Boltzman factor. The minimum number of unpaired electrons that a spectrometer will detect also depends on properties of the paramagnetic system such as the width of the resonance line. The sharp absorption line for the stable free radical α,α-diphenyl-β-picrylhydrazyl is often used to compare the sensitivities of spectrometers. Spectrometers capable of detecting fewer than 10^{12} unpaired electrons (10^{-12} moles) have been built. Because of this high sensitivity, paramagnetic resonance is a promising method for the study of free radical intermediates that occur in many chemical reactions. Concentrations down to 10^{-8} M may be detected with samples of ca. 0.25 ml. assuming a sensitivity of 10^{12} unpaired electrons.

In a free atom with orbital angular momentum, g is given by the familiar Lande formula,[8]

$$g = 1 + \frac{J(J + 1) + S(S + 1) - L(L + 1)}{2J\ (J + 1)} \qquad (2)$$

where L and S are respectively the orbital angular momentum and spin angular momentum and J is the total angular momentum. For L = 0, the case so far considered, g is 2 (when certain quantum electrodynamical corrections are made, the value becomes 2.0023).

In paramagnetic systems of practical interest g-values are usually found to be much nearer the "spin only" value of 2.0023 than that given by the Lande formula. Consider, for example, the Cu^{++} ion in a crystal of $CuSO_4 \cdot 5H_2O$. This ion contains one unpaired d electron ($^2D_{5/2}$), and a g-value of 1.2 is expected for the isolated ion. Experimentally, for the crystal, g-values varying from 2.08 to 2.27 have been found[3] depending on the orientation of the crystal in the applied magnetic field. Electrostatic fields (crystal or ligand fields) from neighboring ions alter the electronic state of the ion. In a free atom, the orbital motion of the electron produces a magnetic field which interacts with the field from the spin (LS coupling). The resultant moment is oriented by an externally applied magnetic field. In the crystal, the electrostatic fields partially destroy or "quench" the magnetism associated with the orbital motion and g-values tend to approach the "spin only" value. Further, the remaining orbital magnetism is "locked" in a direction determined by the crystal field. The spin is oriented along the resultant of the applied field and this internal orbital field. The energy of interaction will depend on the relative directions of these fields and an anisotropic g-value results. The degree of quenching depends on the strength of the crystal field. In systems containing rare earth ions, the unpaired electrons

are in inner shells somewhat shielded from the environment. Deviations from g = 2.0023 can be appreciable. The unpaired electrons of the transition ions are in outer orbitals and interact more strongly with the crystal fields, consequently, quenching is more complete. Orbital magnetism is still more highly quenched in free radicals. Complex organic radicals seldom show as much as one per cent deviation from g = 2.0023. (See, for example, the tabulation of free radical g-values of Wertz.[6]) The unpaired electrons in these substances are in outer orbitals and experience strong quenching forces arising from the electrons in bonding orbitals.

Since most free radicals have g-values close to the free electron value, this property is not very useful for characterizing them. Nuclear hyperfine effects, however, may greatly alter the simple resonance process described above. Hyperfine interactions of the electron with magnetic nuclei cause the absorption line to be split, often into many components. The resulting spectra can be used to identify free radicals and when analyzed in detail give information on the electronic structure of the radical. A nucleus which does not have an even number of neutrons and an even number of protons may possess a spin I and a magnetic moment. This moment will interact with a magnetic field and will assume one of 2I + 1 orientations, each of different energy. The energy states are designated by the nuclear magnetic quantum number M_I = I, I-1, ··· -I. The energy of these states in an external magnetic field and the transitions that occur between them form the subject of nuclear magnetic resonance (NMR). In a paramagnetic resonance experiment, the externally applied field orients the electron spin. It is predominantly the internal magnetic

field from this electron (usually very much greater in magnitude than the externally applied field) that orients a nuclear dipole. Reciprocally, the nuclear dipole produces magnetic fields at the electron position; $2I + 1$ different values are possible depending on the orientation of the nuclear spin. These fields add vectorially to the applied field. Thus, the electron sees a field slightly different from the applied field, and the energy of the electron spin state is changed. In an ensemble of such nuclear spin-electron spin systems, the nuclear levels are very nearly equally populated. The electrons see with essentially equal probability $2I + 1$ different fields, and take $2I + 1$ different energies. This behavior is depicted in Figure 1 for a nucleus of $I = 3/2$. The energies of the two unperturbed electron spin states (the dotted lines of Figure 1) diverge linearly with applied field. The $2I + 1 = 4$ orientations of the nuclear dipole produce internal fields (and energy changes) proportional to M_I. Constant frequency microwave energy produces transitions between the states; the selection rules are such that the M_I do not change when electron spin transitions are induced. Thus, in the example of Figure 1, four equally spaced, equally intense lines occur.

The unpaired electron of a free radical may move in highly delocalized orbitals and hyperfine splittings from many nuclei may occur. For example, the splittings which result from hyperfine interactions involving two nitrogen nuclei are shown in Figure 2. Schematic diagrams of expected splittings are compared with oscilloscope photographs of actual spectra obtained from a crystal containing the free radical α,α-diphenyl-β-picrylhydrazyl (DPPH). Figure 2a represents a

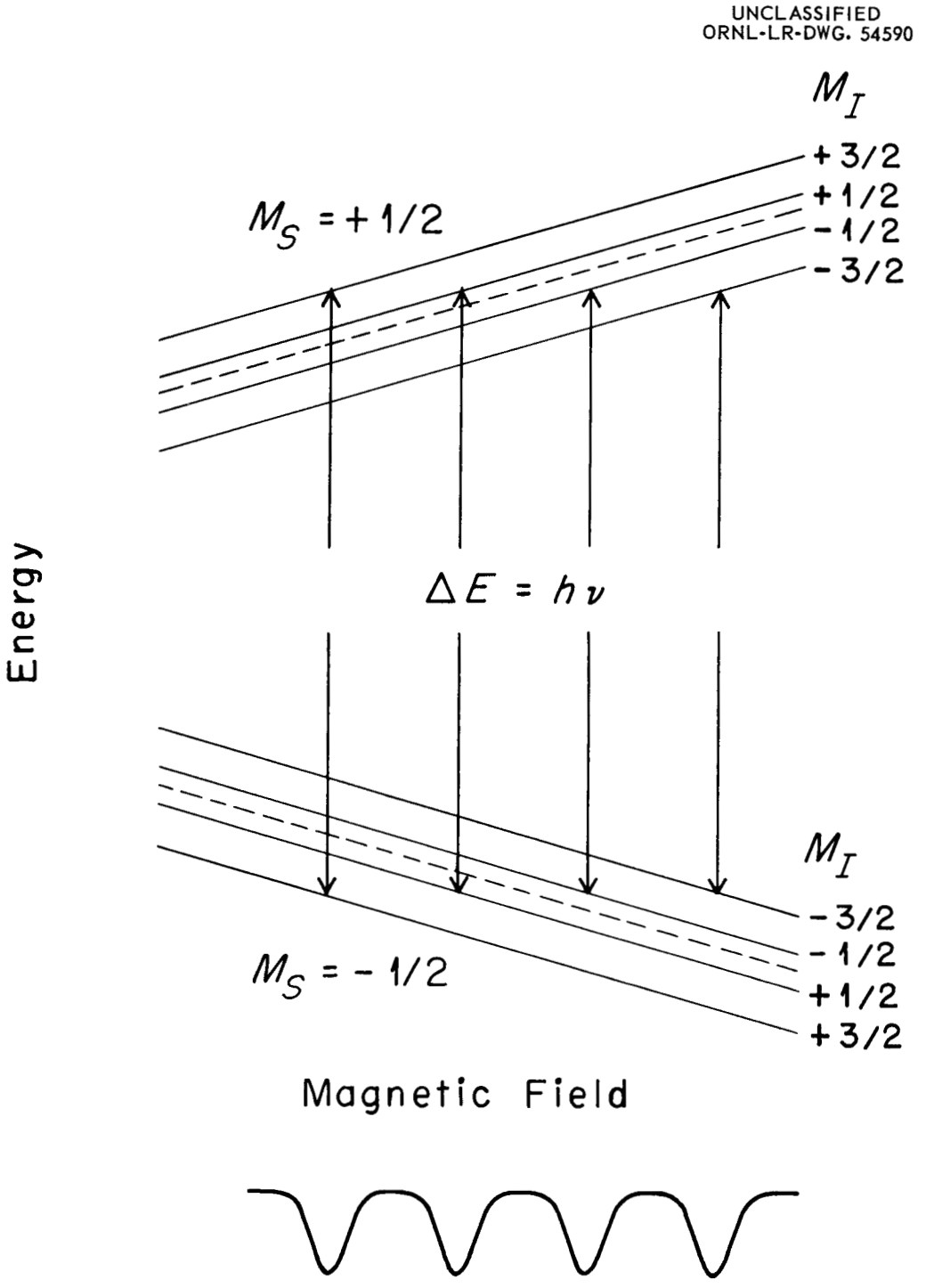

Figure 1. Energy levels and hyperfine spectrum for an unpaired electron ($S = 1/2$) interacting with a nucleus of spin $I = 3/2$.

UNCLASSIFIED
ORNL-LR-DWG. 54591

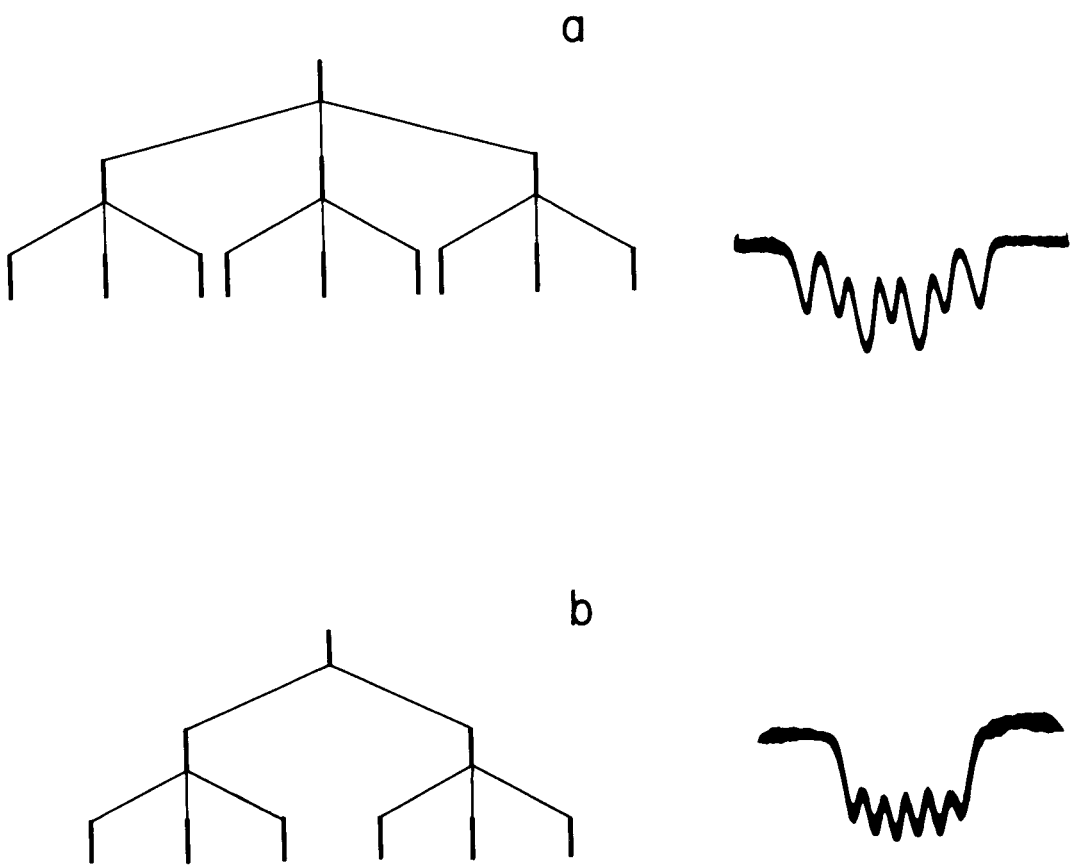

Figure 2. Hyperfine splittings from two nitrogen nuclei in DPPH.
a. Both nuclei are N^{14} ($I = 1$).
b. N^{14} and N^{15} ($I = 1/2$). Same ratio of hyperfine coupling constants.

case in which both nuclei are N^{14} (I = 1) and are unequally coupled with the unpaired electron. One nucleus splits the electron spin resonance line into three widely spaced lines; each of these are then split by the second N^{14} nucleus into three lines somewhat more closely spaced. A nine line spectrum is thus expected. Each of the hyperfine lines actually observed in DPPH are somewhat broadened due to effects which shall be discussed later. As a result, the full nine line multiplicity is not resolved; the closely spaced pairs of Figure 2a appear as single lines of approximately double intensity. Figure 2b represents a similar hyperfine interaction where one of the N^{14} nuclei has been replaced by N^{15} (I = 1/2). Six lines are predicted and are resolved in this case.

The hyperfine splitting from each nucleus is, in general, anisotropic and the amount of splitting can be related to the unpaired electron density near the nucleus. From detailed measurements of the hyperfine line separations, a hyperfine tensor can be evaluated. This tensor may be resolved into two parts. The first, the Fermi or contact term, relates to splittings which are isotropic. These splittings are proportional to the probability $\Psi^2(0)$ of finding the unpaired electron at the nuclear position. From this term, contributions of s orbitals to the unpaired electron wave function can be estimated. The second term, the dipolar term, is related to anisotropic hyperfine separations. It is a measure of the contribution of p, d, etc. orbitals to the electron distribution. Thus, each nucleus which gives rise to discrete hyperfine splittings acts as a probe from which the nature of the wave function of the unpaired electron can be deduced.

Some of the factors affecting the width of a resonance line will now be considered. They are important both because their proper control can improve spectral resolution and because of the information that line width studies can give on the fundamental processes. Each unpaired electron in the crystal sees, in addition to the applied field, an internal magnetic field resulting from the magnetic moments of all the other unpaired electrons in the system. The field from each neighbor depends on its relative position and orientation. The field seen by each electron is different, and hence its energy is different owing to the more or less random orientation of the neighboring electron spins. Each neighbor has essentially equal probability of being oriented parallel or antiparallel to the applied field. Since the separation between adjacent energy values is small, an essentially continuous range of energy states results, and transitions between these states are seen as a broad absorption line. Since the field from a magnetic dipole decreases with the third power of distance, line width arising from this effect is rapidly reduced as the dipoles are separated. For this reason, most paramagnetic resonance studies are carried out in magnetically dilute systems; the paramagnetic molecules are separated by incorporation in a diamagnetic material.

The interaction of the electron with nuclear dipoles (unresolved hyperfine effects) can cause a similar type of broadening. Although nuclear magnetic moments are three orders of magnitude smaller than electron moments, their effects on line width can be appreciable. This type of broadening is particularly evident in hydrogenous materials such as crystalline hydrates and organic free radicals. For example, in many

studies of the paramagnetic transition elements, the ion is incorporated in a crystalline hydrate. Even with extreme magnetic dilution, such that electron dipole interactions are negligible, rather broad lines (ca. 6 gauss) remain. This type of nuclear dipolar broadening can be reduced, however, by making appropriate isotopic replacements. For example, the magnetic moment of the deuteron is about one-third of that of the proton and line widths from this effect are proportionately reduced when the substitution is made.

Paramagnetic species often give much sharper lines in solution than would be expected from the foregoing considerations. Those interactions that cause anisotropy and many of those that give width to a paramagnetic resonance line are angularly dependent such that the average of these contributions over all directions in space is zero. In solution the paramagnetic species undergo a tumbling motion. If this motion is sufficiently rapid, the above interactions are not seen. Often, with non-viscous solvents, extremely sharp lines are observed. Dipolar contributions to hyperfine splittings are similarly absent; only the isotropic (contact) part contributes. Much of the paramagnetic resonance work on organic free radicals has been carried out in solution. Often this is the only type of observation that has been made because of the difficulty in incorporating the radical in a suitable single crystal. In some respects, this type of study has an advantage over a comparable study in a single crystal. The narrower lines observed in solution afford much greater spectral resolution; consequently weak hyperfine interactions, not resolved in crystals, can often be distinguished and studied. On the

other hand, information available from the dipolar interaction is lost, and often it is this information which is most definitive of the unpaired electron distribution. It should also be mentioned that useful studies can sometimes be made using amorphous or polycrystalline solids. There are systems (e.g. irradiated biological systems) which cannot be studied in solution or in single crystals. In such cases, a broad line lacking in structure may result because of anisotropic variations in g-value and hyperfine structure. In other cases, however, the g anisotropy is small and the contribution to the hyperfine structure comes largely from the isotropic terms. Consequently sufficient detail can be resolved so that useful information regarding the nature of the radical species can be inferred.

There is another interaction, again involving the unpaired electrons, that can cause drastic changes in the character of the paramagnetic resonance line. This is the exchange narrowing process. If two or more paramagnetic molecules are sufficiently close together that the wave functions of their unpaired electrons appreciably overlap, quantum mechanical exchange forces must be considered. Although the amount of exchange may be negligible in comparison to that which occurs in chemical bonding, it can cause drastic changes in spin resonance spectra. An extreme narrowing of the line may occur in concentrated free radicals. For example, crystals of the free radical diphenyl picrylhydrazyl would be expected to show a line width of the order of 50 gauss on the basis of electron dipolar broadening; yet the observed line width (full width at half height) is only one or two gauss. Usually,

but not necessarily, exchange effects decrease more rapidly with separation of the radicals than do the electron dipolar interactions.

Fundamental to the width of any spectral line are the lifetimes of the states between which transitions occur. The uncertainty in energy of a state is related to its lifetime through the uncertainty principle $\Delta E \Delta t = \hbar$. When the life of a state is short the uncertainty in energy is correspondingly large. The spin-lattice relaxation process has been mentioned earlier. The spin lattice relaxation time, a measure of the lifetime of a spin state, varies widely in paramagnetic crystals and increases rapidly with decreasing temperature. In some paramagnetic crystals (particularly the rare earths) the thermal relaxation time is so short that lines are broadened to an extent that observations at room temperature cannot be satisfactorily made; very low temperatures are necessary to avoid broadening of these absorption lines through rapid spin-lattice relaxation. Most complex free radicals, however, have sufficiently long spin-lattice relaxation times so that the lines are not drastically broadened by this process at room temperature. Another way in which the lifetime of a spin state may be limited is through chemical reaction. Changes in line width from this cause have been used to study very rapid exchange reactions involving free radicals in solution.[9]

B. Previous Work on DPPH

The purpose of the investigation reported here is to characterize the spin resonance spectra of a particular free radical α,α-diphenyl-β-

picrylhydrazyl (DPPH)

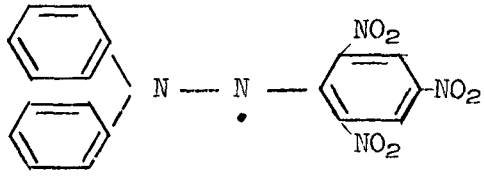

and from this to draw conclusions about the distribution of the unpaired electron throughout the molecule.

The stable free radical DPPH was first prepared by Goldschmidt and Renn[10] in 1922. This intensely violet colored material can be prepared in pure form and shows little tendency to dimerize to the tetrazane. Measurements of the bulk magnetic susceptibility[11] on the solid have demonstrated this stability down to 83°K.

DPPH has received a large amount of attention from those interested in paramagnetic resonance. Selwood[12] states, "This compound ... has become so popular with the paramagnetic resonance specialists that there is some question as to what they would do without it." Its resonance was first reported simultaneously by Holden, Kittel, Merritt and Yager[13] and by Townes and Turkevitch.[14] A single sharp absorption line with a g-value[13] of 2.0036 and 2.7 gauss half width (full width at half height) was observed in polycrystalline DPPH. The narrowness of the line was attributed to intermolecular exchange effects (exchange narrowing).

Numerous investigations of the paramagnetic resonance of single crystals of DPPH have been made. The g-value was found[15] to vary from 2.0035 to 2.0041 depending on the crystal orientation. The closeness of these values to the free electron g-value and the small anisotropy is typical of complex free radicals and indicates that the orbital angular

momentum is highly quenched. Small anisotropies in the line width have also been observed;[16,17] the half-width varied, with orientation, from 1.5 gauss to 2.1 gauss. Measurements of the g-value as a function of microwave frequency[18] up to 75,000 Mc are in accord with the values[15] at lower frequencies; the tensor describing the anisotropy in g was found to be axially symmetric. The g-value anisotropy at low temperatures was found to be slightly greater than at room temperature.[19] Detailed measurements of the line shape from powdered DPPH have been made.[20] Small differences in the line width have been seen in DPPH crystallized from different solvents.[21]

DPPH is widely used as a reference material in paramagnetic resonance studies. Its sharp absorption line of accurately known g-value is used as a secondary standard for the determination of the g-value of other paramagnetic centers. Because it can be prepared in pure form and is quite stable, it is also used as an intensity standard for determining the number of unpaired electrons in paramagnetic systems. In this respect, the material is also often used to compare the sensitivities of various paramagnetic resonance spectrometers. Their sensitivities vary with the width of the resonance line.

DPPH gives a single sharp resonance line in solutions of high concentration similar to that seen in solid material. With dilution, the interactions contributing to exchange narrowing decrease; the line broadens and ultimately a characteristic five line hyperfine spectrum is resolved.[12,15,19,22,23,24] Photographs of the paramagnetic resonance spectrum of DPPH in dilute solution as displayed on an oscilloscope are

shown in Figure 3. Figure 3a is that of normal DPPH, and Figure 3b is that of DPPH labelled with N^{15} in the β nitrogen position. The partially resolved, symmetric, five line spectrum (Figure 3a) has been interpreted as being due to the hyperfine coupling of the unpaired electron with the two hydrazyl nitrogens.[15,22] In general, such an interaction with two N^{14} nuclei (I = 1) would yield a nine line spectrum. If the couplings to the two nitrogen nuclei are nearly equal, some of the lines will superimpose (within their line widths) and a five line spectrum will result. A recent analysis[25] of the spectrum indicates that the ratio of the coupling constants is 0.82. It was not possible to determine whether the α or β nitrogen had the greater hyperfine interaction, since both interacting nuclei were identical. The solution spectra of other free radicals of the hydrazyl structure have been investigated. Although the spectral patterns are considerably different in appearance, they all may be explained by the hyperfine interaction of two N^{14} nuclei. In one $((C_6H_5)_2\ N\dot{N}\ (C_6H_2)(NO_2)_2\ SO_3Na)$ the full nine line multiplicity was resolved.[22,26] The separation between the partially resolved nitrogen hyperfine lines of DPPH in solution has been reported to be ca. 10 gauss.[15] This amount of contact interaction, when assumed to come from an unpaired electron in nitrogen 2s orbitals, accounts for only a few per cent of the unpaired electron density.

Resonance lines from hydrogens are often seen in free radicals containing aromatic groups. Because of the absence of such lines in DPPH, it has been thought that the unpaired electron is strongly localized on the two hydrazyl nitrogens. Recently,[27] however, spectra of DPPH in highly

UNCLASSIFIED
ORNL-LR-DWG. 54592

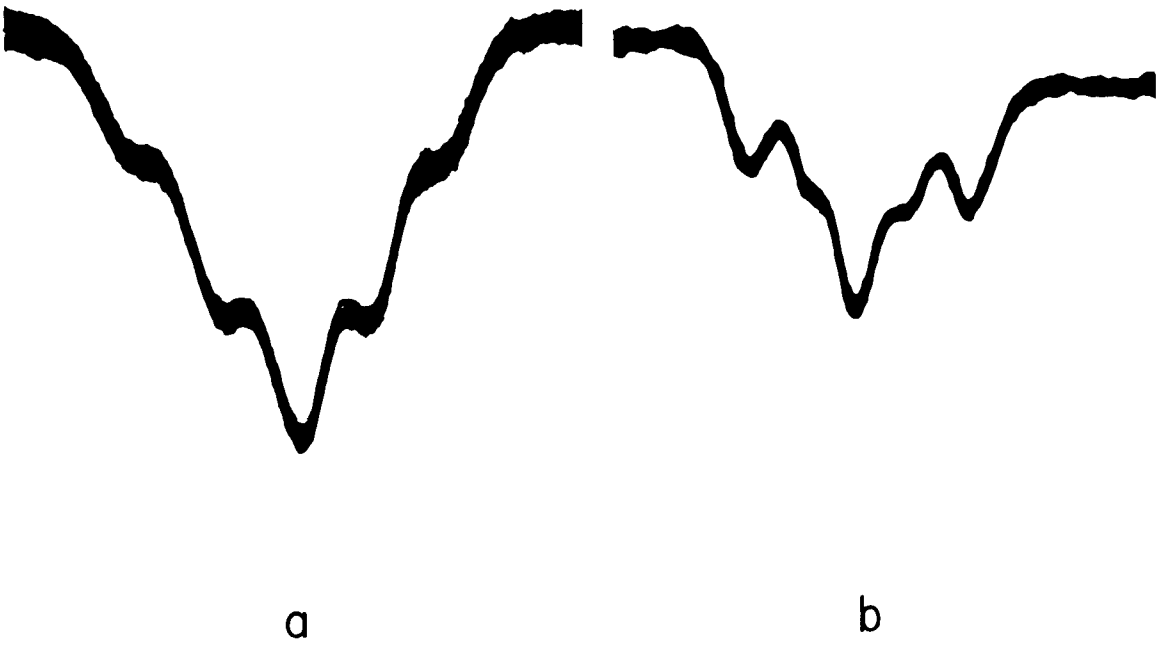

Figure 3. Paramagnetic resonance spectra from dilute DPPH solutions.
a. DPPH of normal isotopic content.
b. DPPH in which the β hydrazyl nitrogen was N^{15}.

purified, oxygen free solvents have been obtained in which proton hyperfine lines are resolved. Well over one hundred closely spaced lines were seen; the spectrum was not interpreted.

It was the purpose of this investigation to study the paramagnetic resonance spectrum of DPPH in single crystals, to resolve from this spectrum both the contact and dipolar contributions to the hyperfine interaction, and from this to deduce some of the detail of the unpaired electron distribution. It was necessary to magnetically dilute DPPH in a diamagnetic single crystal so that dipolar broadening effects and exchange effects would not obscure the spectrum. The diamagnetic "parent" of DPPH, α,α-diphenyl-β-picrylhydrazine ($DPPH_2$) was chosen as the host crystal. Because of the structural similarity of the two molecules, it was thought that dilute solid solutions of DPPH in $DPPH_2$ might be easily prepared. Experiments were performed on crystals of normal isotopic content and on crystals in which the β hydrazyl nitrogen was replaced with N^{15}. It was found that labelled crystals not only gave more useful spectra because of the fewer lines and consequently greater resolution, but also allowed the hyperfine interactions from the α and β nitrogens to be distinguished.

CHAPTER II

EXPERIMENTAL

A. Preparation of Materials

Both $DPPH_2$ and DPPH of normal isotopic content were obtained commercially. The $DPPH_2$ was obtained from the Eastman Kodak Company, and the DPPH from the Aldrich Chemical Company. The N^{15} labelled compounds were synthesized. The syntheses, carried out first with normal materials to test the procedures, are described in terms of the following reactions ($N^* = N^{15}$):

$$HN^*O_3 + NaOH \rightarrow NaN^*O_3 + H_2O \quad (1)$$

$$NaN^*O_3 + Pb \rightarrow NaN^*O_2 + PbO \quad (2)$$

$$(C_6H_5)_2NH + HN^*O_2 \rightarrow (C_6H_5)_2NN^*O + H_2O \quad (3)$$

$$(C_6H_5)_2NN^*O + 4(H) \xrightarrow[HOAc]{Zn} (C_6H_5)_2NN^*H_2 + H_2O \quad (4)$$

$$(C_6H_5)_2NN^*H_2 + Cl(C_6H_2)(NO_2)_3 \rightarrow (C_6H_5)_2NNH \text{ Picryl} + HCl \quad (5)$$

$$(C_6H_5)_2NN^*H \text{ Picryl} \xrightarrow{PbO_2} (C_6H_5)_2NN^* \text{ Picryl} \quad (6)$$

Reaction 1. Nitric acid containing 98.3 per cent N^{15} was obtained from the Isotope Division of the Oak Ridge National Laboratory. It was converted to sodium nitrate by neutralizing with sodium hydroxide and was evaporated to dryness.

Reaction 2. The conversion of the nitrate to nitrite presented some difficulties. Although the direct thermal decomposition of an alkali nitrate is a "textbook reaction", several attempts to prepare sodium nitrite by this method were unsuccessful. The thermal decomposition of

sodium nitrate was found to be extremely slow at temperatures just above its melting point; when heated much hotter the decomposition was accompanied by the evolution of oxides of nitrogen. This reaction has been discussed recently by K. J. Mysels.[28] D. F. Heath[29] has investigated this decomposition in the presence of lead, and has found that the conditions under which the reaction is carried out, particularly the mesh size of the lead, are critical if high yields of nitrite are to be had. The mesh size recommended by Heath (60-80 mesh) was not available. We have found that good yields of nitrite can be obtained if a large excess of granular lead is used and the reaction mixture is heated for prolonged periods of time in an inert atmosphere. A mixture of 5.8 g. of NaN^*O_3 and 38 g. of granulated lead was heated for 16 hr. under an argon atmosphere at 380°. After cooling, the sodium nitrite was leached from the matrix with hot water. A small aliquot was analyzed; an 80 per cent yield was found.

Reactions 3 and 4. The directions of Clusius and Vecchi[30,31] for preparing labelled unsymmetrical diphenylhydrazine were followed. A solution containing 9 g. of diphenylamine, 65 ml. of absolute ethanol, and 6.5 ml. of concentrated hydrochloric acid was cooled to -5° and the NaN^*O_2 solution (3.7 g. NaN^*O_2) was added slowly. After about one hour, N-nitrosodiphenylamine was precipitated by adding excess water; it was separated from the solution and dried. Diphenylhydrazine was prepared by slowly adding acetic acid to a cold alcoholic solution of the N-nitrosodiphenylamine in which zinc dust was suspended. The solution was separated from the excess zinc; the hydrazine was precipitated as the hydrochloride and dried. A yield of 62 per cent based on the NaN^*O_2 was obtained.

Reactions 5 and 6. Procedures of Porier, Kahler, and Benington[32] were followed. About one-half (3.5 g.) of the labelled diphenylhydrazine hydrochloride in ethanol was treated with sodium bicarbonate and picryl-chloride. The mixture was boiled gently to speed the reaction. Chloroform was added to dissolve the $DPPH_2$ and the mixture was filtered. The solution was concentrated by partial evaporation of the solvent, and ethanol was added to precipitate the $DPPH_2$. A yield of ca. 40 per cent was obtained. Part of the $DPPH_2$ was converted to the free radical DPPH by treating it with an excess of lead dioxide in benzene. After filtration, the benzene solution was concentrated by partial evaporation of the benzene and n-hexane added to precipitate the DPPH. The yield was not determined.

B. Growth and Properties of Crystals

Crystals of $DPPH_2$, grown from benzene solution, were chosen as the diamagnetic medium in which to incorporate the free radical DPPH. Preliminary experiments indicated that $DPPH_2$ would incorporate small amounts of DPPH and that resolved paramagnetic resonance lines could be observed. Pure DPPH had previously been found[33] to crystallize from benzene in a monoclinic form; the space group is Pc and there are two molecules of DPPH plus two of benzene in the unit cell. It was found from x-ray powder patterns* that crystals of $DPPH_2$ grown from benzene

---

*The author wishes to thank R. D. Ellison of the Oak Ridge National Laboratory Chemistry Division for the x-ray examinations reported in this thesis.

solution had a different space group. It was necessary to determine the symmetry and cell parameters of $DPPH_2$ so that the paramagnetic resonance measurements could be referred to known crystal axes and related to the crystal symmetry. An investigation to deduce these parameters was undertaken by R. D. Ellison and the author.[34] Small crystals of $DPPH_2$ were grown by evaporation of a benzene solution and single crystal x-ray diffraction patterns were taken. The small crystals, which contained benzene of crystallization, required special care to prevent decomposition while obtaining the diffraction patterns. They were mounted in thin wall capillaries that contained a benzene saturated atmosphere. The cell parameters determined from the single crystal data were refined using powder patterns. It was found that $DPPH_2$ crystals are monoclinic and of space group $P2_1$. The cell dimensions are: $a = 9.37$ Å, $b = 10.78$ Å, $c = 11.87$ Å; the monoclinic angle is $111^\circ\ 14'$. The benzene of crystallization was directly determined from loss of weight on heating freshly crystallized material to constant weight at 60°. The density of the crystals was determined pycnometrically. From these data and from the cell size it was found that the crystals contained two molecules of $DPPH_2$ plus two of benzene in the unit cell. Powder patterns of pure $DPPH_2$ crystals and those containing small amounts of DPPH were compared; no differences were observed.

Rather large crystals (several millimeters on an edge) were required for the paramagnetic resonance work. This was necessary in order to get signals of adequate intensity and yet have the crystals sufficiently dilute in DPPH that exchange and dipolar broadening effects

would not interfere. Attempts were made to grow these crystals by slow evaporation of benzene solutions. A nearly saturated solution of $DPPH_2$ containing an appropriate amount of DPPH was placed in a partially covered vessel and the solvent was allowed to evaporate slowly for a week or more at room temperature. Ordinarily only masses of small crystals were obtained with this method. Presumably, on evaporation, the solutions first became supersaturated and then showered many small seeds.

A thermal gradient method was found to be more reliable. In a typical experiment, about one-half to one gram of $DPPH_2$ was placed in the bottom of a 15 ml. test tube and 10 ml. of benzene containing ca. 20 mg. of DPPH was added. The upper part of the tube was first heated gently for a few hours while the lower part was kept cool in a water bath. This treatment was designed to dissolve any small seeds in the upper part of the tube. A small seed crystal glued to a glass rod with polyvinyl alcohol was then immersed a few centimeters below the solution level. The bottom end of the tube was then heated in an oven at ca. 60°; the upper part was unheated. Saturated solution from the bottom was carried upward by thermal convection and crystallization occurred in the cooler regions near the top. With luck, after many days, a seed grew into a well-developed single crystal of sufficient size and DPPH content to be experimentally useful. In some instances well-developed crystals formed on the cool sides of the test tube without the use of a seed crystal. The technique was by no means foolproof; often the growth was polycrystalline or twinned. Since only a few well-developed crystals were needed for

the study, no particular effort was made to refine or improve the procedure. The usual difficulties attendant to growing crystals were amplified because of the small amount of labelled compounds available, and because the opacity of the solution prevented day by day observation of the progress of crystal growth. The largest single crystal obtained weighed about one-half gram. As noted above, the crystals tended to lose benzene of crystallization. Large crystals lost benzene slowly and could be handled for several hours in air without appreciable decomposition. When stored for long periods, they were placed in a desiccator containing a benzene saturated atmosphere.

It was desirable to determine the morphology of the $DPPH_2$ crystals so that they might easily be oriented for the paramagnetic resonance observations. While these orientations could have been made with x-rays, this technique is time consuming and would have been further complicated by the deterioration of the crystals due to loss of benzene. Interfacial angles of a large well-developed crystal were measured using a Unicam two circle optical goniometer. The faces were indexed by comparing these data with angles calculated from the cell parameters determined by x-rays. The interfacial angles observed optically agreed with the calculated values to ca. 0.5° or less. This uncertainty is due primarily to roughness of the crystal faces; the light beam reflected from these faces was somewhat diffuse and angles could not be measured with high precision. Faces with the following Miller indices were found to develop: 001, 100, 011, $01\bar{1}$, 110, $10\bar{1}$, $11\bar{1}$, $1\bar{1}0$, $\bar{1}11$. The first four were usually predominant and determined the characteristic shape of the crystal.

The amount of DPPH incorporated in the crystal varied, of course, with the conditions of crystal growth. In a typical experiment using the thermal gradient method (20 mg. DPPH, 1 g. $DPPH_2$, and 10 ml. benzene) crystals containing of the order of 0.1 per cent DPPH were obtained. This concentration gave paramagnetic resonance lines of adequate intensity and yet was sufficiently dilute that dipolar broadening and exchange narrowing effects could be ignored. A conventional assay of this small amount of DPPH in a crystal would have been difficult. It was done in a semiquantitative manner by comparing the intensities of the resonance lines from the crystal with those of a benzene solution containing a known amount of DPPH.

It was necessary to label both the DPPH and the $DPPH_2$ when growing the N^{15} labelled crystals. If the $DPPH_2$ was not labelled, a rapid exchange of the β hydrogen of the $DPPH_2$ to the DPPH would destroy the labelling. An attempt was made to measure the rate of this exchange. Labelled DPPH and normal DPPH each give a characteristic resonance spectrum in solution (Figure 3). A small amount of labelled DPPH was dissolved in benzene and its spectrum observed. A saturated solution of normal $DPPH_2$ was added and the solutions were mixed. Even though a lapse of less than one minute had occurred before the spectrum of the mixture could be observed the spectrum had changed to that of normal DPPH. Thus, the exchange occurred in less than one minute.

Attempts have been made to incorporate DPPH into $DPPH_2$ crystals grown from other solvents and into N-picryl-9-aminocarbazine which has a structure very similar to $DPPH_2$. All such attempts have so far proved unsuccessful. $DPPH_2$ will crystallize from carbon disulfide

solution in small needlelike crystals; attempts to grow satisfactorily large crystals by the evaporation or thermal gradient methods failed. Similarly, chloroform as a solvent has failed to yield satisfactory crystals. Large, well formed crystals have been grown from acetone, but there was not sufficient DPPH incorporated into these crystals to be experimentally useful even though very high DPPH-$DPPH_2$ ratios were used in solution. Similarly, N-picryl-9-aminocarbazine, while producing large, well developed crystals from benzene, failed to incorporate sufficient DPPH.

With this latter system, the exchange reaction between DPPH and the carbazine was briefly investigated. The free radical carbazyl (N-picryl-9-aminocarbazyl) gives a characteristic solution spectrum.[7] If the DPPH were to abstract the β hydrogen of N-picryl-9-aminocarbazine, the carbazyl radical would be formed and a characteristic change in spectrum should occur. An excess of the carbazine was added to a small amount of DPPH dissolved in benzene. Unlike the rapid exchange between DPPH and $DPPH_2$, no exchange occurred. The spectrum did not change from that of pure DPPH in three months at room temperature.

C. Spectrometer

A transmission type spectrometer design by Dr. Ralph Livingston and built at the Oak Ridge National Laboratory was used in this investigation. The spectrometer operates at microwave frequencies of about 9000 Mc (x-band). The essential features are shown in Figure 4.

UNCLASSIFIED
ORNL-LR-DWG. 54593

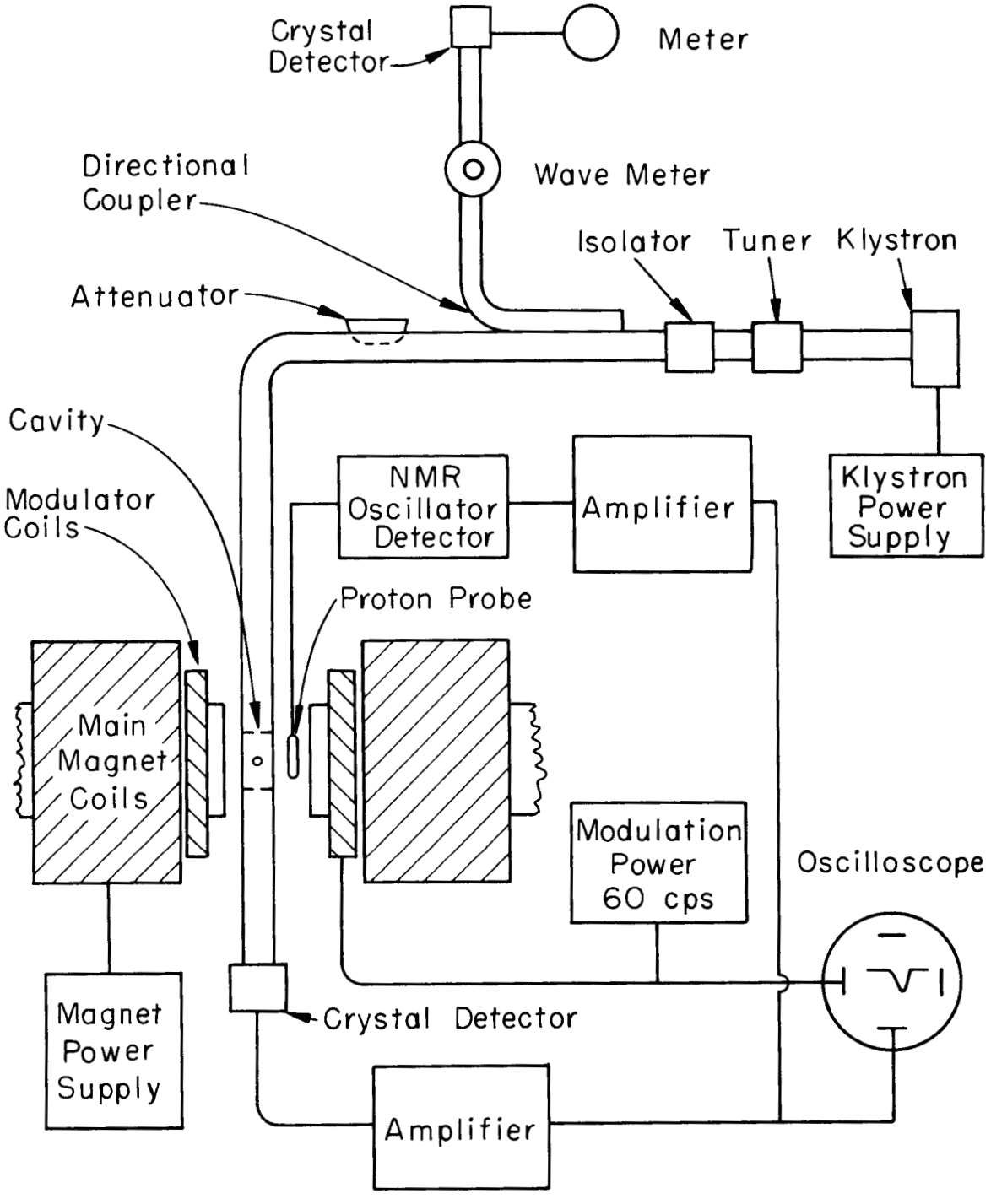

Figure 4. Schematic diagram of a paramagnetic resonance spectrometer.

Microwave power, produced by a klystron oscillator, is propagated through a waveguide to a resonant cavity between the poles of an electromagnet. This cavity contains the paramagnetic sample. The energy transmitted through the cavity is detected by a silicon crystal diode, amplified, and fed to the vertical plates of an oscilloscope. The magnet is equipped with two sets of coils. Power for the main magnet coils is obtained from a dc supply and regulated to provide a steady magnetic field. This field is adjustable; in the experiments reported here fields near 3000 gauss were used. Smaller modulation coils add an alternating component to the steady field. Power for these modulation coils is furnished from a line at 60 cps, and controlled with a variable transformer. At full line voltage (115 volts) the amplitude of the oscillation of this field is about 100 gauss. The horizontal sweep of the oscilloscope is synchronized with this alternating field. The steady field is adjusted so that the 60 cps field excursions will sweep back and forth over the resonance line. In this manner, the paramagnetic resonance spectrum is displayed on the oscilloscope; the horizontal deflection represents magnetic field, and the vertical deflection represents the amount of absorption of microwave power by the sample.

Included in the microwave circuit are a load isolator, a tuner, attenuators, and a wavemeter circuit. The isolator, a ferrite device, allows free passage of the microwaves from the klystron to the system but effectively prevents transmission in the reverse direction. This prevents reflected energy from pulling or detuning the klystron. The tuner is used to match the output of the klystron to the transmission

line. Attenuators are used to control the amount of power falling on the sample. The wavemeter circuit is used to determine the frequency of the microwaves. A directional coupler samples a small portion of the microwave energy and conducts it to the wavemeter which is a cylindrical resonant cavity with one movable end which can be controlled by means of a micrometer screw. Since the resonant frequency of a cavity depends on the cavity dimensions, the micrometer is calibrated directly in frequency units. The calibration of the wavemeter used is reliable to one or two parts in 10^4 (about 1 Mc out of 9000 Mc).

The sample cavity is a brass rectangular cavity having inside dimensions of 0.4 x 0.9 x 0.95 inches. It is operated in the TE_{101} mode. (The electromagnetic modes of microwave cavities are described in standard references on microwave electronics; see e.g. Gintzon.)[35] The cavity is resonant at a fixed microwave frequency. Paramagnetic resonance transitions result from the interaction of the electron spin with the magnetic component of the microwave electromagnetic oscillations. This component is at maximum strength near the top and the bottom of the cavity operating in the TE_{101} mode. Thus, samples are placed in these positions to obtain maximum signal intensity. The cavity is not connected directly to the waveguide as indicated in Figure 4, but is coupled to the waveguide by short lengths of coaxial cable. This permits the cavity to be placed in a dewar flask so that observations can be made at low temperatures if desired.

Experimental measurements were made with the crystals oriented so that the applied magnetic field was parallel to the ac, ab and bc

crystallographic planes. The ab and bc crystal faces were well developed and provided a convenient method of orientation for measurements in these planes; the appropriate face was placed on the bottom of the cavity which was aligned accurately parallel to the magnetic field. The direction of the field was altered by rotating the entire magnet assembly. It was still necessary to define the field direction relative to the crystal axes in a particular plane. It was possible to take advantage of the crystal symmetry to determine these angles. The hyperfine separations in these planes were expected to be symmetric with respect to the orientation in which the field is parallel to the b axis; i.e., if we define this angle arbitrarily as 0°, then hyperfine spacings observed at a given positive angle will be identical with those at the same negative angle. (See Figures 10 and 11). The crystals were placed in the cavity so that the b axis was approximately parallel to the applied magnetic field. This was done by aligning appropriate crystal edges parallel to the cavity walls. A series of measurements were then made at angles on both sides of this position. From these data, and from the symmetry, the orientation of the axes with respect to the applied field was deduced.

This technique could not be used for measurements in which the field was parallel to the ac plane. The ac crystal face was not found to develop, and there were no symmetry conditions which defined angles in this plane. A thin brass rod was glued to the crystal so that the rod was normal to the ac plane; the optical goniometer was used to effect this orientation. The crystal was then inserted into the cavity through a small hole in the top with the brass rod held vertically and

normal to the applied field direction. The brass rod was indexed with a marker parallel to the c axis so that this direction could be defined. This direction could also be determined by comparing data taken in the ac and bc planes. The intersection of these planes is the c axis.

Magnetic field measurements were made with a small proton probe and a nuclear magnetic resonance oscillator-detector. The probe was a small coil surrounding an ampoule of water. Radiofrequency power at ca. 13.5 Mc was supplied from the oscillator; a nuclear magnetic resonance transition of the proton was excited, detected and also fed to the vertical plates of the oscilloscope. Thus, a sharp marker (the proton resonance line) appeared on the oscilloscope simultaneously with a paramagnetic resonance line. The radiofrequency was adjusted until the two lines were superimposed. The frequency was then measured using an Army Signal Corps BC-221 frequency meter. The magnetic field strength was computed from this frequency and the accurately known gyromagnetic ratio of the proton. The conversion of frequency ν_h to field strength H is given by[36]

$$H = \nu_h \times 10^{-3}/4.25776 \qquad (3)$$

This equation can be used directly to determine the separations between hyperfine lines. Accurate absolute field measurements were needed to compute g-values, however, and a small correction was necessary. The position of the proton probe and the position of the paramagnetic sample were not identical. Slightly different fields occurred at these positions because of small inhomogeneities in the magnetic field. This difference was determined by measuring the line position of a small sample of powdered DPPH whose g-value is accurately known (2.0036). The absolute

field at the sample position was calculated using Equation 1 and compared with the field at the proton probe position. The correction was of the order of 1 part in 10^3.

CHAPTER III

EXPERIMENTAL RESULTS

A. Theory

The energy states of a paramagnetic system, between which electron spin resonance transitions occur, can be represented by a spin Hamiltonian developed by Abragam and Pryce.[37] The various terms entering into this Hamiltonian have been discussed by the above authors, by Bleaney and Stevens[2] and others. For the particular problem of interest here, the hyperfine spectra of DPPH magnetically diluted in a single crystal of $DPPH_2$, the following Hamiltonian is appropriate:

$$\mathcal{H} = - g\beta\left[\vec{H}\cdot\vec{S} + \vec{S}\cdot A_\alpha\cdot\vec{I}_\alpha + \vec{S}\cdot A_\beta\cdot\vec{I}_\beta\right] . \qquad (4)$$

Here g is the spectroscopic splitting factor, β is the Bohr magneton, $\vec{S}$ and $\vec{I}$ are the electron and nuclear spin operators in units of $\hbar$, and A, the hyperfine tensor, is a rank two symmetric tensor whose detailed form will be considered later. The subscripts α and β designate the interacting nuclei. For the present problem they designate the α and β nitrogens of α,α-diphenyl-β-picrylhydrazyl. It should be emphasized here that Equation 4 is a spin Hamiltonian. Only interactions involving the electron and nuclear spins are considered. In principle, the elements of the hyperfine tensors can be determined from the spatial parts of the wave function of the unpaired electron, but for a complicated molecule such as DPPH a theoretical computation of this type is not feasible. Thus, it shall be the purpose here to solve the spin Hamiltonian so that the

elements of the hyperfine tensors may be evaluated from the paramagnetic resonance spectra. Later, we shall use these values to deduce some of the detail of the unpaired electron wave function.

The first term $(\vec{H}\cdot\vec{S})$ represents the interaction of the electron spin with the applied magnetic field (the Zeeman energy). In general, this term should reflect the anisotropic behavior of the g-value and have the form $\vec{S}\cdot\underset{\sim}{g}\cdot\vec{H}$ where $\underset{\sim}{g}$ is a rank two symmetric tensor. As will be discussed later, experimental g-values were found to be very nearly independent of angle, hence the isotropic form given above where g is a scalar is adequate. The hyperfine terms $(\vec{S}\cdot A\cdot\vec{I})$ represent the magnetic interaction of the nuclear and electron spin dipoles. In general, one hyperfine term is required for each interacting nucleus. Anticipating the experimental findings, only two are included in the Hamiltonian.

Two terms that might contribute to hyperfine effects have been omitted from the Hamiltonian. These are the term representing the quadrupole interaction and a term of the form $\vec{H}\cdot\vec{I}$ representing the interaction of the nuclear spin with the applied field. Both of these contributions are small compared to the hyperfine terms and can be neglected in the present problem. The hyperfine energy (ca. 100 Mc.) is small compared to the Zeeman energy (ca. 9000 Mc. at 3000 gauss) and can be treated as a small perturbation. The solution given below will be based on the treatment of Trammell, Zeldes, and Livingston.[38]

We shall consider first only the first term of the Hamiltonian and calculate zero order energies unperturbed by hyperfine interactions. The electron spin $\vec{S}$ interacts with the applied field and is quantized

with respect to this direction; i.e. the component of $\vec{S}$ in the field direction $\vec{S}\cdot\vec{H}/H$ has eigenvalues $M_s = \pm 1/2$. It follows directly that

$$E_o = -g\beta H M_s, \tag{5}$$

where H is the magnitude of $\vec{H}$. This equation represents the energy levels of a spin-only electron in a magnetic field. These levels diverge linearly with the field strength as indicated by the dashed lines of Figure 1. The hyperfine energy, according to first order perturbation theory, is

$$E_1 = -g\beta \left\langle \vec{S}\cdot A_\alpha\cdot\vec{I}_\alpha + \vec{S}\cdot A_\beta\cdot\vec{I}_\beta \right\rangle . \tag{6}$$

Integrations over the electron spin and nuclear spin variables of the zero order wave functions are indicated by the angular brackets. It will not be necessary to express these functions explicitly, since the solution of Equation 6 follows simply from the properties of the spin vectors. From the zero order treatment, the expectation of $\vec{S}$ is

$$\langle S \rangle = M_s \vec{H}/H = M_s\vec{h}, \tag{7}$$

where $\vec{h}$ is a unit vector in the field direction. Thus,

$$E_1 = -g\beta M_s \left\langle \vec{h}\cdot A_\alpha\cdot\vec{I}_\alpha + \vec{h}\cdot A_\beta\cdot\vec{I}_\beta \right\rangle . \tag{8}$$

To integrate over the nuclear variables, it was recognized that $\vec{I}$ is quantized in the direction of the vector $\vec{V} = \vec{h}\cdot A$. The component of $\vec{I}$ in this direction $\vec{I}\cdot\vec{V}/V$ has eigenvalues M_I. Thus,

$$\langle I \rangle = M_I \vec{V}/V, \tag{9}$$

where M_I is the nuclear magnetic quantum number and V is the magnitude of $\vec{V}$. Equation 8 then becomes

$$\begin{aligned} E_1 &= -g\beta M_s\left[M_{I\alpha}\frac{\vec{V}_\alpha\cdot\vec{V}_\alpha}{V_\alpha} + M_{I\beta}\frac{\vec{V}_\beta\cdot\vec{V}_\beta}{V_\beta}\right] \\ &= -g\beta M_s\left[M_{I\alpha}V_\alpha + M_{I\beta}V_\beta\right] . \end{aligned} \tag{10}$$

Since

$$V = (\vec{V}\cdot\vec{V})^{\frac{1}{2}} = (\vec{h}\cdot A\cdot A\cdot\vec{h})^{\frac{1}{2}} = (\vec{h}\cdot A^2\cdot\vec{h})^{\frac{1}{2}} \tag{11}$$

where $A^2 = A\cdot A$ is again a symmetric rank-two tensor, the hyperfine energy is

$$E_1 = -g\beta M_s\left[M_{I\alpha}(\vec{h}\cdot A^2_\alpha\cdot\vec{h})^{\frac{1}{2}} + M_{I\beta}(\vec{h}\cdot A^2_\beta\cdot\vec{h})^{\frac{1}{2}}\right] . \tag{12}$$

The total energy, $E_0 + E_1$, is given by

$$E = -g\beta M_s\left[H + M_{I\alpha}(\vec{h}\cdot A^2_\alpha\cdot\vec{h})^{\frac{1}{2}} + M_{I\beta}(\vec{h}\cdot A^2_\beta\cdot\vec{h})^{\frac{1}{2}}\right] . \tag{13}$$

The allowed transitions[38] are $\Delta M_s = 1$ and $\Delta M_I = 0$. Thus,

$$\Delta E = g\beta H + g\beta\left[M_{I\alpha}(\vec{h}\cdot A^2_\alpha\cdot\vec{h})^{\frac{1}{2}} + M_{I\beta}(\vec{h}\cdot A^2_\beta\cdot\vec{h})^{\frac{1}{2}}\right] . \tag{14}$$

The spacings, in magnetic field units (gauss), of the hyperfine components from the unperturbed line position (center of the symmetric hyperfine multiplet corresponding to all $M_I = 0$ in the above equation) are given by

$$\Delta H = M_{I\alpha}(\vec{h}\cdot A^2_\alpha\cdot\vec{h})^{\frac{1}{2}} + M_{I\beta}(\vec{h}\cdot A^2_\beta\cdot\vec{h})^{\frac{1}{2}} . \tag{15}$$

When referred to the principal axes of the hyperfine tensors, Equation 15 becomes

$$\Delta H = M_{I\alpha}\left[\sum_i h_i^2\ A_{ii}^2\right]^{\frac{1}{2}}_\alpha + M_{I\beta}\left[\sum_j h_j^2\ A_{jj}^2\right]^{\frac{1}{2}}_\beta , \tag{16}$$

where the h's are direction cosines of the applied magnetic field with respect to the principal axes (not necessarily the same for both tensors), and the A's are written in component form. In the diagonal representation,

$$(A_{ii})^2 = (A^2)_{ii} . \tag{17}$$

These equations describe the number of hyperfine lines and the anisotropic behavior of their spacings. The nuclear magnetic quantum numbers M_I take $2I + 1$ values (I, $I - 1$, ... $- I$) for each nucleus. Thus, each of the electron spin levels designated by $M_s = +\frac{1}{2}$ or $-\frac{1}{2}$ are split into

$(2I_\alpha + 1)(2I_\beta + 1)$ levels. Since the various M_I do not change when the electron spin transition is induced, the same number of hyperfine lines is expected. In normal DPPH both nitrogens are N^{14} ($I_\alpha = I_\beta = 1$) and nine lines are expected. In the labelled compound the β nitrogen is N^{15} ($I_\beta = \frac{1}{2}$) and six lines are expected. The field dependence of the energy levels shown in Figure 1 is based on Equation 13.

The DPPH-$DPPH_2$ system was expected to have a somewaht more complicated hyperfine spectrum than predicted by Equations 15 and 16. The space group of $DPPH_2$ is $P2_1$. Assuming that the incorporation of DPPH into $DPPH_2$ does not destroy this symmetry, there are two crystallographically equivalent positions in the unit cell for it to enter. These positions are related by a two-fold screw axis parallel to the crystallographic b axis. The hyperfine spectra will come from two DPPH molecules, each of which is oriented differently with respect to the applied field. The α-nitrogen, for example, is characterized by two hyperfine tensors A_α^2 and A_α^{*2} corresponding to each DPPH molecule in the unit cell. They are related by the point symmetry of the $DPPH_2$ crystal. In matrix notation

$$A_\alpha^{*2} = \tilde{C}_2 \, A_\alpha^2 \, C_2 \tag{18}$$

where C_2 represents a two-fold rotation about the b axis. A similar expression relates the β-tensors. When the magnetic field is parallel to the crystallographic ac plane $\vec{h}\cdot A^2\cdot\vec{h} = \vec{h}\cdot A^{*2}\cdot\vec{h}$, and a multiplicity characteristic of a single molecule is expected. With the magnetic field in other directions, the hyperfine splittings are different ($\vec{h}\cdot A^2\cdot\vec{h} \neq \vec{h}\cdot A^{*2}\cdot\vec{h}$) and eighteen lines are expected for the two DPPH molecules with

a two N^{14} hyperfine interaction; similarly, twelve lines are expected for the labelled molecule. It should be noted that no new useful information is obtained from the additional lines because the tensors of the two molecules are related by known crystal symmetry.

B. General Features of Spectra

Spectral observations and measurements were made on the normal (N^{14}-N^{14}), and labelled (N^{14}-N^{15}) crystals. In both cases resolved hyperfine lines were found to have a full width at half height of about 7 gauss. The lines were found to power saturate. This was particularly evident when observations were made at liquid nitrogen temperature.

At each field setting a g-value was determined using Equation 1 and measured values of the microwave frequency and magnetic field strength. Since the g-value refers to the Zeeman splitting unperturbed by hyperfine effects, field values corresponding to the center of the symmetric hyperfine multiplet were required. These were determined by averaging measured field values for the extreme lines (high field and low field) of the spectrum. As indicated in Chapter II, corrections for field differences at the proton probe and the sample were made using pure powdered DPPH. The g-values for the labelled radical are presented in Table I; they average 2.003 with an angular variation of about ± 0.001. This is essentially the same as has been found for pure DPPH crystals. Because of the essential constancy of these values, the first term in the Hamiltonian (Equation 4) can be considered to be isotropic.

As expected from the $DPPH_2$ crystal symmetry, the hyperfine spectra were complicated by the presence of two molecules of DPPH in the unit cell. In the ac plane, however, both molecules appeared magnetically equivalent and spectra typical of one DPPH molecule were observed. In this plane, the normal (N^{14}-N^{14}) crystals gave, at certain angles, a maximum of nine resolved lines while the labelled (N^{14}-N^{15}) crystals gave a maximum of six lines. Typical spectra* in this plane are shown in Figures 5 and 6. The change in multiplicity from nine lines with the normal to six lines with the labelled compound indicates that the hyperfine spectra come from the hydrazyl nitrogens.

Spectra of labelled DPPH with the magnetic field parallel to the ab crystallographic plane are shown in Figure 7 and with the field parallel to the bc plane in Figure 8. The width of the lines was comparable to the line spacings in these planes, and, generally, spectral resolution was poor. The outermost lines, however, were sufficiently resolved that significant results could be inferred from their behavior. When the magnetic field was rotated from a direction parallel to the ac plane to a direction skew to this plane, it was expected that each hyperfine line would split into two equivalent lines because of the presence of the two DPPH molecules. This splitting was observed with the outer lines, but could not be observed elsewhere because of the poor resolution. The spacings between these lines were in accord with the

---

*Spectra shown in this thesis are reproductions of photographs of the oscilloscope screen taken with a Land oscilloscope camera. The enlargement of these photographs is variable, hence they should not be compared quantitatively. Spectra displayed on the oscilloscope may be somewhat distorted from their true shape due to instrumental effects.

UNCLASSIFIED
ORNL-LR-DWG. 54594

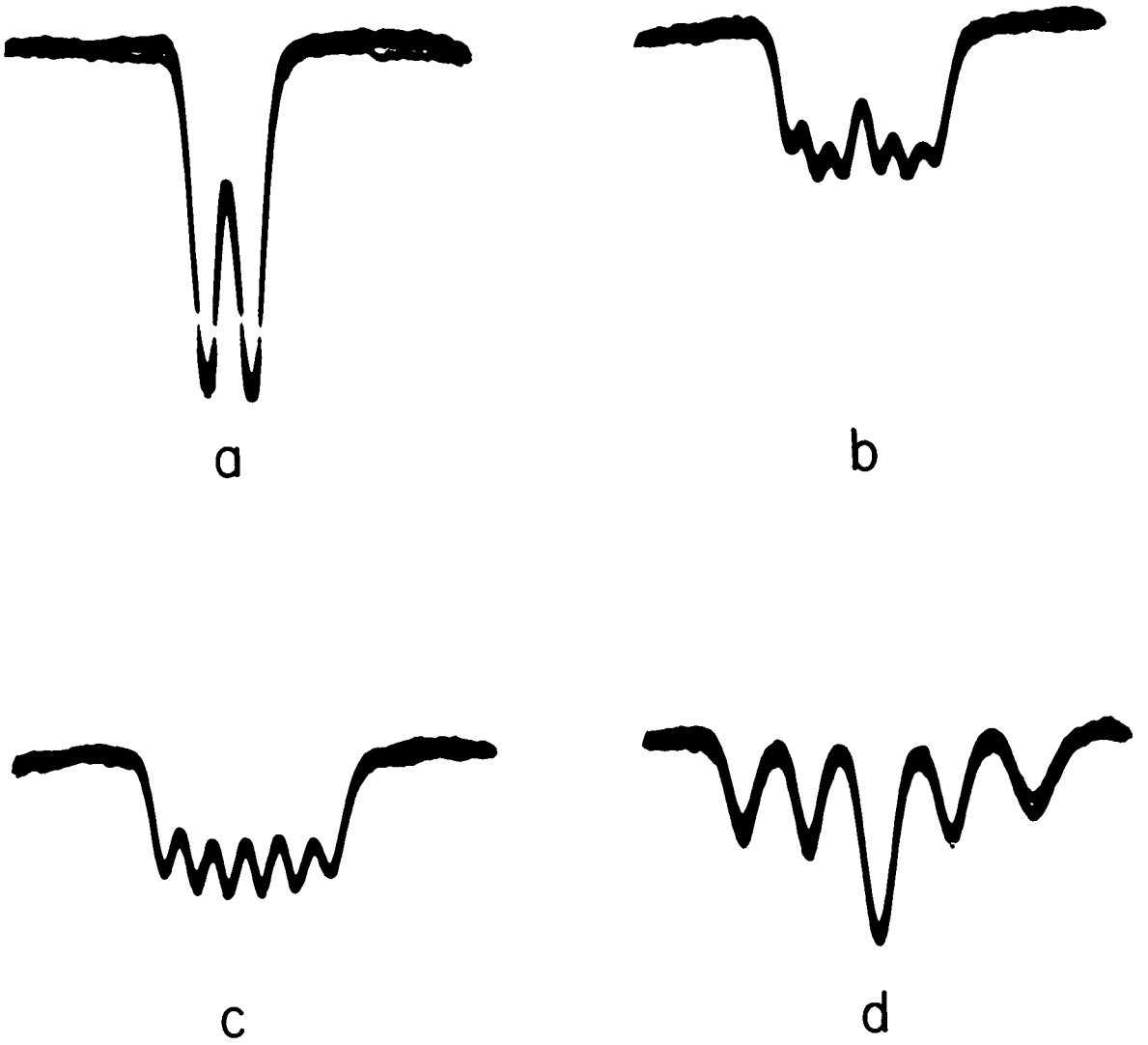

Figure 5. Spectra of a single crystal containing N^{15} labelled DPPH. The magnetic field was parallel to the ac plane. Field directions relative to the c axis: (a) 70°, (b) 45°, (c) 40°, and (d) 0°.

UNCLASSIFIED
ORNL-LR-DWG. 54595

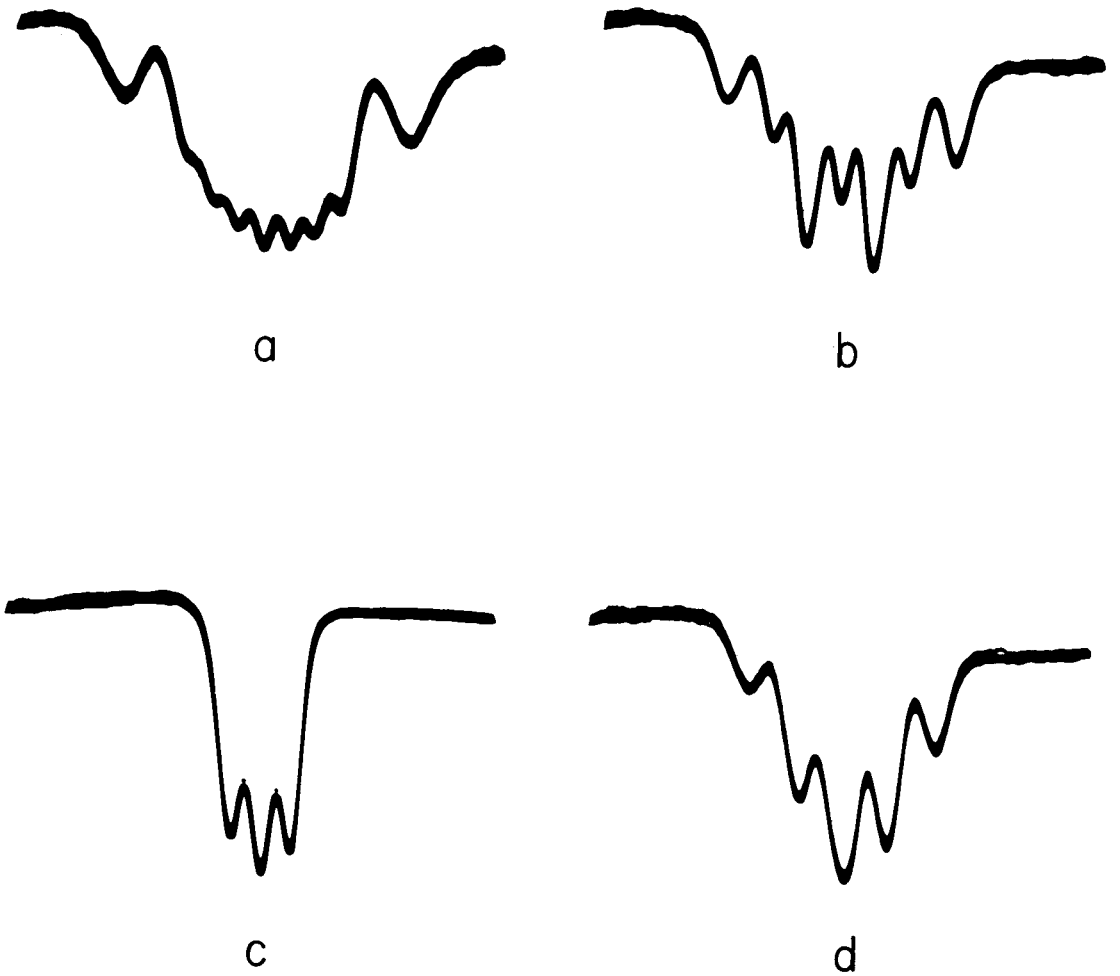

Figure 6. Spectra of a single crystal containing normal DPPH. The magnetic field was parallel to the ac plane. Field directions relative to the c axis are (a) 170°, (b) 20°, (c) 70°, (d) 135°.

UNCLASSIFIED
ORNL-LR-DWG. 54596

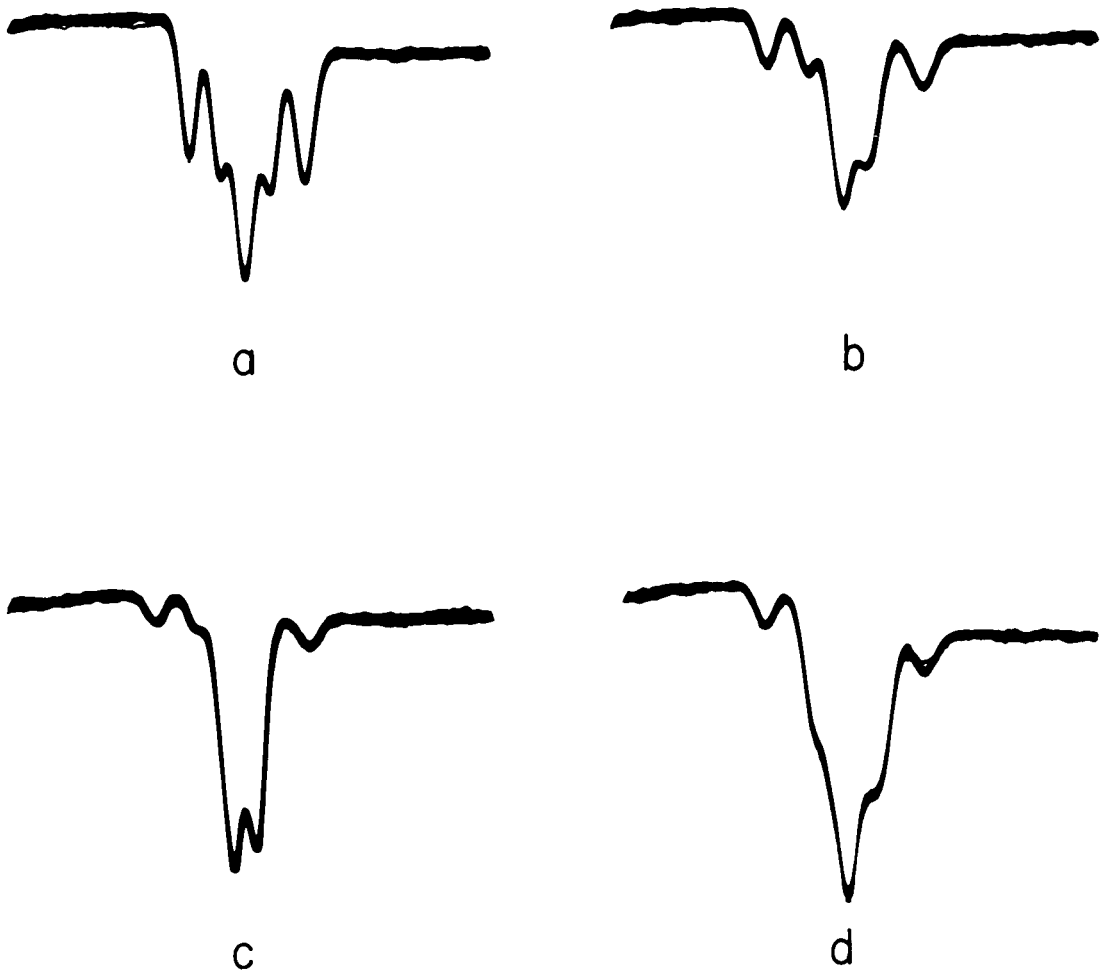

Figure 7. Spectra of a single crystal containing N^{15} labelled DPPH. The magnetic field was parallel to the ab plane. Field directions relative to the a axis : (a) 0°, (b) 54°, (c) 126°, (d) 150°.

UNCLASSIFIED
ORNL-LR-DWG. 54597

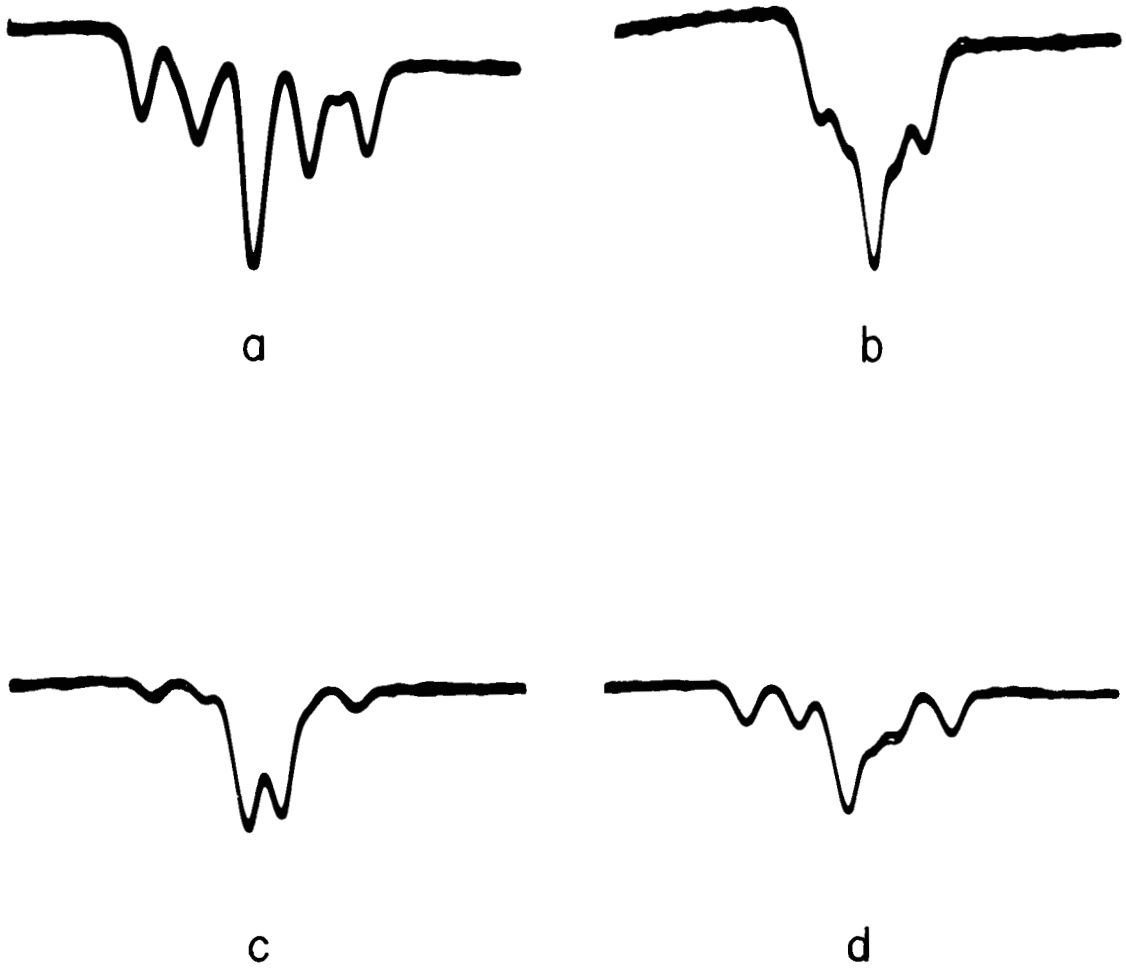

Figure 8. Spectra of a single crystal containing N^{15} labelled DPPH. The magnetic field was parallel to the bc plane. Field directions relative to the c axis are (a) 17°, (b) 90°, (c) 125°, (d) 55°.

crystal symmetry; the intensities were not. One line was about one-third the intensity of the other. This effect was noted with several crystals (both normal and labelled). The effect could not be attributed to any asymmetry in the experimental configuration and we are forced to conclude that there are different numbers of DPPH molecules in each of the crystallographically "equivalent" positions. This is not strictly consistent with the space group for $DPPH_2$. Only small amounts of DPPH were contained in the $DPPH_2$ crystals and distortions may have been present that were not observed with x-rays. Presumably, even with small amounts of added DPPH, the host lattice does not accommodate it well, and there are distortions not seen by x-rays at such low concencentrations; the "symmetry related positions" are not occupied with equal probability. This might be expected from the finding that 2 per cent DPPH (compared to $DPPH_2$) had to be placed in solution to obtain a crystal containing only ca. 0.1 per cent DPPH.

C. Evaluation of Hyperfine Tensors

The data obtained from the labelled DPPH crystals were used to evaluate the hyperfine tensors. These data are tabulated in Table I and presented graphically in Figures 9-11. Since only the β-nitrogen was labelled with N^{15}, an unambiguous assignment of the two hyperfine tensors to the appropriate nitrogens was possible. The use of the labelled crystals had a further advantage. Because of fewer lines, compared to the normal material, spectral lines were resolved over a much greater range of angle, thus giving more reliable data to use in evaluating the

TABLE I

MEASURED HYPERFINE SPACINGS AND G-VALUES FOR LABELLED DPPH

Crystal Orientation*			G-value	Hyperfine Spacings in Gauss**					
a	b	c		$-1,-\frac{1}{2}$	$0,-\frac{1}{2}$	$1,-\frac{1}{2}$	$-1,\frac{1}{2}$	$0,\frac{1}{2}$	$1,\frac{1}{2}$
ac plane									
107	90	4	2.0027	-32.2	-17.3			17.7	32.2
97	90	14	2.0023	-30.0	-17.0	-2.9	3.8	16.3	29.9
92	90	19	2.0027	-28.0	-15.6	-3.3	3.7	16.2	28.1
87	90	24	2.0029	-26.4	-15.0	-3.4	4.0	15.6	26.3
82	90	29	2.0027	-24.4	-14.1	-3.7	4.3	14.2	24.3
77	90	34	2.0026	-22.6	-13.5	-4.4	3.9	13.3	22.5
67	90	44	2.0024	-18.0	-11.2	-5.2	4.8	11.0	18.0
42	90	69	2.0038	- 5.3	- 5.3	-5.3	5.3	5.3	5.3
7	90	104	2.0033	-18.2					18.2
13	90	124	2.0037	-27.0	-12.4			13.6	27.0
33	90	144	2.0034	-32.3	-15.8			15.4	35.3
53	90	164	2.0029	-34.0	-17.3			18.1	34.1
ab plane									
9	81	110	2.0028	-22.8					22.8
14	76	110	2.0034	-24.0					24.0
19	71	109	2.0036	-25.1					25.1
19	71	109	2.0034	-25.0					25.0
29	61	108	2.0034	-26.1					26.1
39	51	106	2.0033	-26.6					26.6
44	46	105	2.0029	-26.5					26.5
49	41	103	2.0028	-26.2					26.2
59	31	100	2.0032	-25.0					25.0
69	21	97	2.0031	-23.4					23.4

TABLE I (CONTINUED)

Crystal Orientation*			G-value	Hyperfine Spacings in Gauss**					
a	b	c		$-1,-\frac{1}{2}$	$0,-\frac{1}{2}$	$1,-\frac{1}{2}$	$-1,\frac{1}{2}$	$0,\frac{1}{2}$	$1,\frac{1}{2}$
ab plane									
79	11	94	2.0032	-20.8					20.8
129	39	78	2.0027	-25.6					25.6
129	39	78	2.0025	-26.0					26.0
134	44	76	2.0029	-26.0					26.0
139	49	74	2.0029	-25.9					25.9
139	49	74	2.0029	-26.4					26.4
144	54	73	2.0025	-26.3					26.3
149	59	72	2.0028	-25.8					25.5
154	64	71	2.0029	-25.7					25.7
159	69	71	2.0032	-25.3					25.3
159	69	71	2.0036	-25.3					25.3
169	79	70	2.0022	-22.4					22.4
179	89	69	2.0039	-21.0					21.0
bc plane									
90	88.5	1.5	2.0030	-33.0					33.0
90	73.5	16.5	2.0029	-36.0					36.0
90	73.5	16.5	2.0035	-27.0					27.0
90	68.5	21.5	2.0028	-36.1					36.1
90	68.5	21.5	2.0037	-24.1					24.1
90	58.5	31.5	2.0026	-36.3					36.3
90	56	34	2.0023	-36.2					36.2
90	48.5	41.5	2.0024	-35.2					35.2
90	49	41	2.0023	-35.5					35.5
90	46	44	2.0023	-34.9					34.9
90	44	46	2.0017	-34.6					34.6

TABLE I (CONTINUED)

Crystal Orientation*			G-value	Hyperfine Spacings in Gauss**					
a	b	c		$-1,-\frac{1}{2}$	$0,-\frac{1}{2}$	$1,-\frac{1}{2}$	$-1,\frac{1}{2}$	$0,\frac{1}{2}$	$1,\frac{1}{2}$
bc plane									
90	38.5	51.5	2.0029	-33.4					33.4
90	34	56	2.0021	-31.6					31.6
90	28.5	61.5	2.0029	-30.0					30.0
90	24	66	2.0024	-28.2					28.2
90	14	76	2.0026	-24.3					24.3
90	9	81	2.0026	-22.1					22.1
90	1	91	2.0033	-17.2					17.2
90	6	96	2.0027	-19.3					19.3
90	11	101	2.0028	-22.6					22.6
90	16	106	2.0029	-25.0					25.0
90	26	116	2.0025	-29.1					29.1
90	31.5	121.5	2.0030	-31.3					31.3
90	36	126	2.0023	-32.3					32.3
90	41.5	131.5	2.0027	-34.0					34.0
90	51.5	141.5	2.0027	-35.8					35.8
90	61.5	151.5	2.0026	-36.4					36.4
90	71.5	161.5	2.0028	-36.1					36.1
90	71.5	161.5		-26.0					26.0
90	76.5	166.5	2.0027	-35.3					35.3
90	76.5	166.5	2.0035	-28.2					28.2

*Angles in degrees of applied magnetic field with respect to crystallographic axes.

**The hyperfine lines are designated by the nuclear magnetic quantum numbers $M_{I\alpha}$, $M_{I\beta}$.

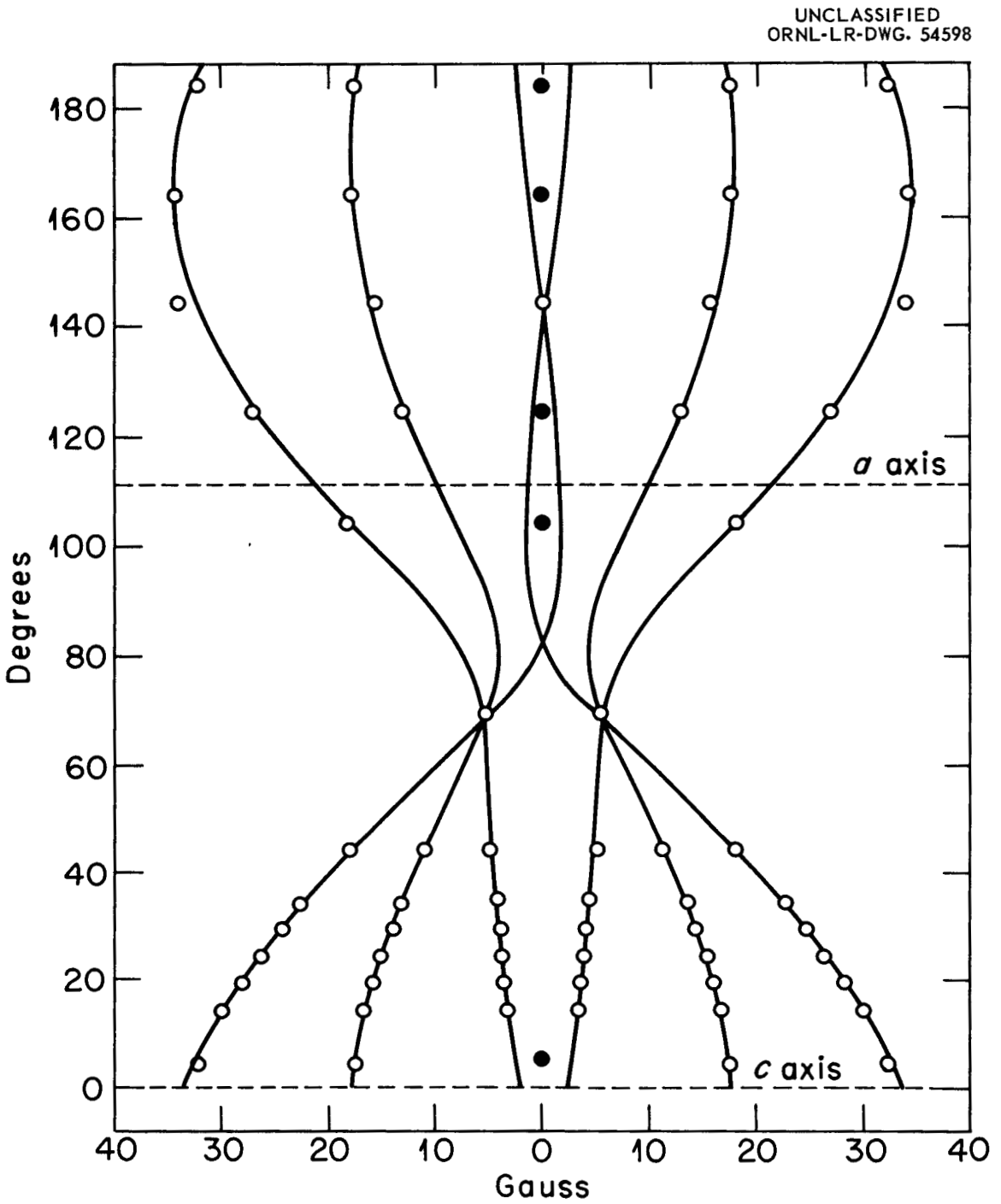

Figure 9. Measured values and calculated curves for the hyperfine separations in a single crystal containing N^{15} labelled DPPH. The magnetic field was parallel to the ac plane. Dark circles represent unresolved lines.

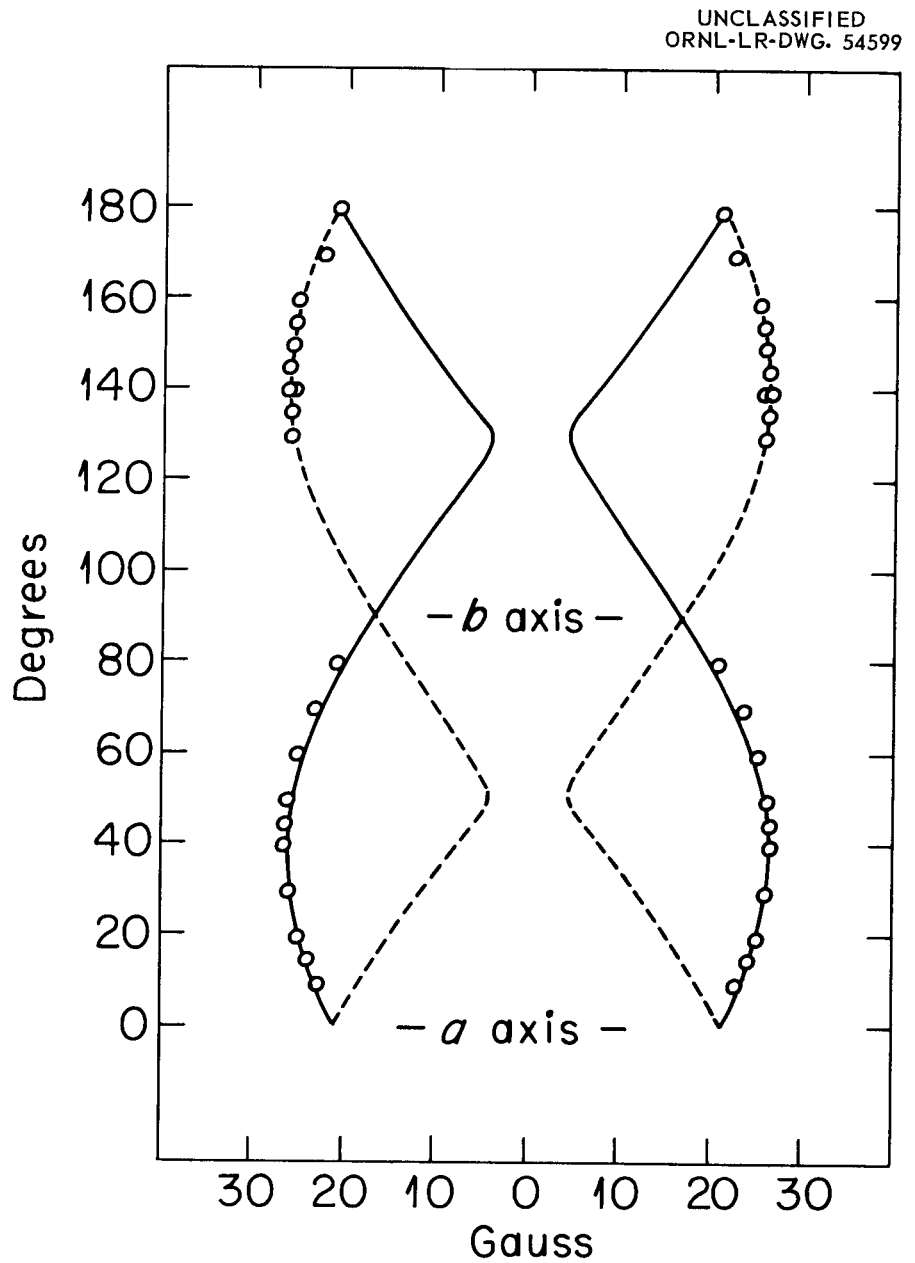

Figure 10. Measured values and calculated curves for the overall hyperfine separations in a single crystal containing N^{15} labelled DPPH. The magnetic field was parallel to the ab plane. The solid and dotted curves represent the two symmetry related molecules.

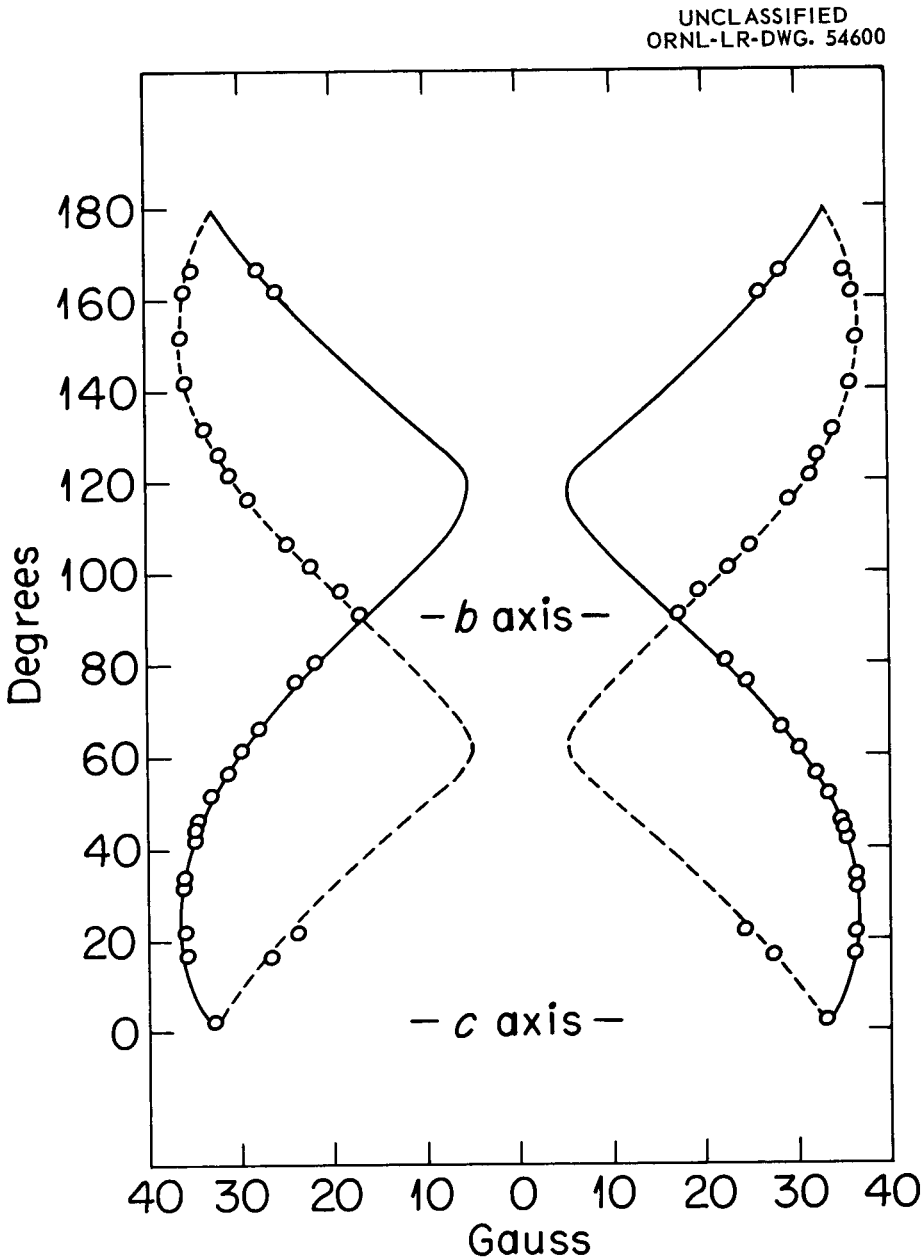

Figure 11. Measured values and calculated curves for the overall hyperfine separations in a single crystal containing N^{15} labelled DPPH. The magnetic field was parallel to the bc plane. The solid and dotted curves represent the two symmetry related molecules.

tensors. Indeed, it is doubtful if the tensors could have been evaluated from data obtained with the normal crystals. Measured values of the hyperfine splittings from the normal (N^{14}-N^{14}) crystals were found to agree well with those calculated from the tensors deduced from the spectra of the labelled crystals when appropriate corrections for the nuclear spin and nuclear magnetic moments were made. This comparison is shown graphically in Figure 12.

Fitting the data of this problem required the evaluation of twelve parameters; i.e. six elements of A_α^2 and six elements of A_β^2 (the tensors are symmetric). Attempts were made to compute these parameters by methods based on Equation 15. To define the applied field direction $\vec{h}$, a cartesian axis system based on the $DPPH_2$ crystal axes was chosen (see Figure 13). Two of the axes were the b and c crystallographic axes; the third, the a* axis, was chosen to be orthogonal to b and c and to lie in the ac plane. For computational purposes, Equation 15 may be written as follows:

$$\Delta H_t = 2\Delta H_\alpha + 2\Delta H_\beta \tag{19}$$

$$\Delta H_\alpha = (\vec{h}\cdot A_\alpha^2\cdot\vec{h})^{\frac{1}{2}} \tag{20}$$

$$\Delta H_\beta = (\vec{h}\cdot A_\beta^2\cdot\vec{h})^{\frac{1}{2}}/2 \tag{21}$$

The quantities ΔH_t, ΔH_α, and ΔH_β are defined by the hyperfine line separations indicated in Figure 14. When the magnetic field was parallel to the ac plane the lines were resolved sufficiently well that the individual hyperfine spacings ΔH_α and ΔH_β could be measured. The field, when parallel to this plane, has no component along b. Equation 20, written

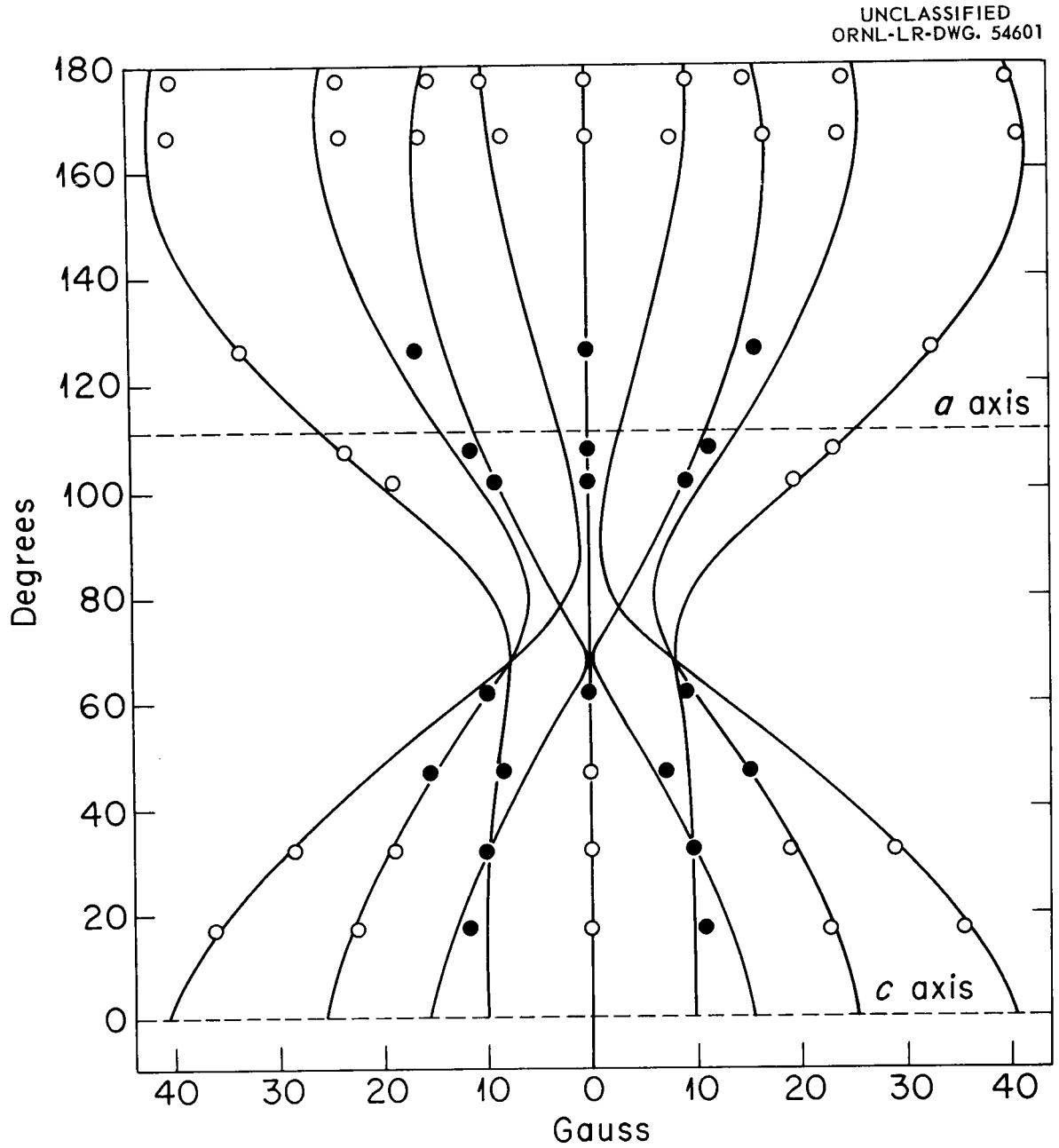

Figure 12. Measured values and calculated curves for the hyperfine separations in a $DPPH_2$ crystal containing normal DPPH. The magnetic field was parallel to the ac plane. The solid circles represent unresolved lines.

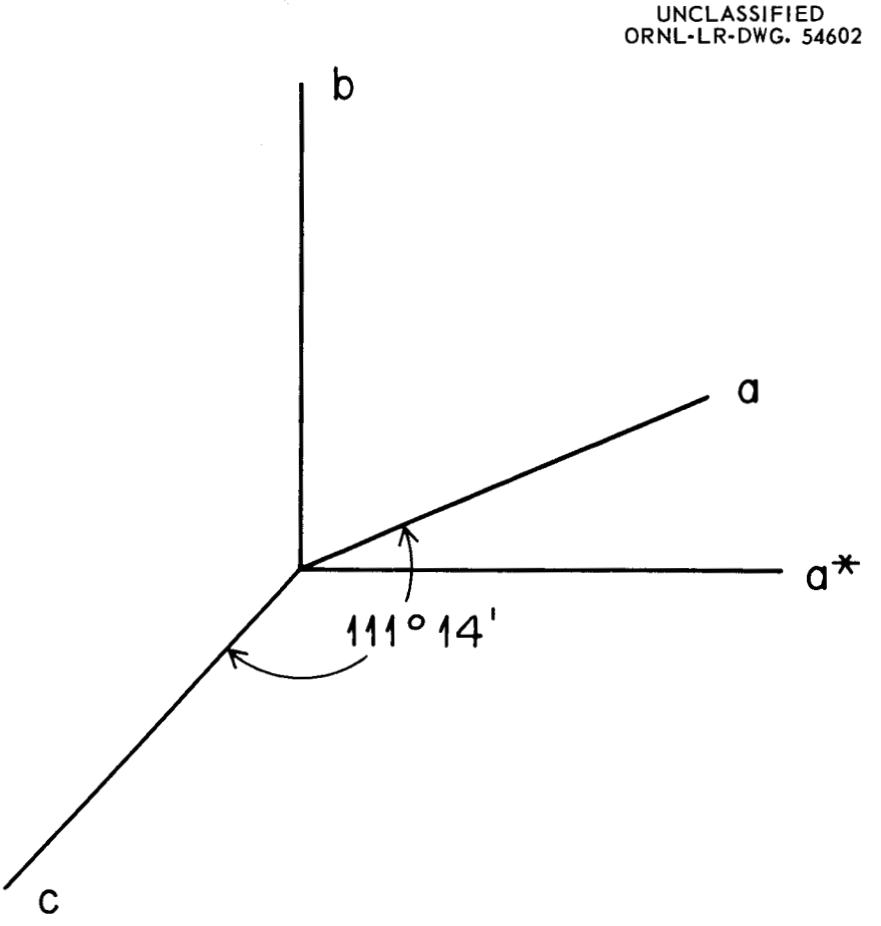

Figure 13. Axis system used in evaluating hyperfine tensors. The monoclinic axes of $DPPH_2$ are a, b, and c. An orthogonal set a*, b, and c was used to define the magnetic field direction.

UNCLASSIFIED
ORNL-LR-DWG. 54603

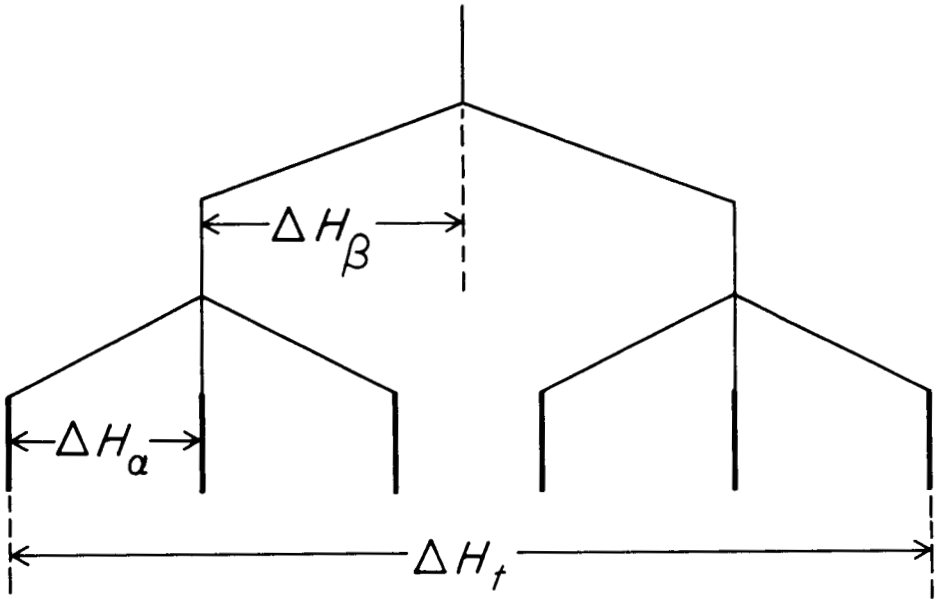

Figure 14. Schematic diagram of 6 line hyperfine spectrum defining ΔH_α , ΔH_β , and ΔH_t .

in component form, is then

$$\Delta H_\alpha^2 = h_1^2\ (A_\alpha^2)_{11} + h_3^2\ (A_\alpha^2)_{33} + 2h_1h_3(A_\alpha^2)_{13}\ , \qquad (22)$$

where h_1 and h_3 are, respectively, the components of $\vec{h}$ (direction cosines) with respect to the a and c axes. The angles tabulated in Table I were used to calculate h_1 and h_3. The three tensor elements of Equation 22 were deduced from these and the observed values of ΔH_α. A similar set of elements was calculated for the tensor using values of ΔH_β.

The evaluation of the other three elements of each tensor required data from the ab and bc crystallographic planes. Because of the poor spectral resolution in these planes, the only reliable data that could be obtained were the overall splittings of the hyperfine patterns ΔH_t. (The outer lines were generally sufficiently resolved that this measurement could be made reliably). The sum of the contributions of the individual nitrogens contribute to this parameter. The contributions from each tensor are not directly separable (see Equations 19-21). Evaluating the six remaining elements by hand computations would have been a formidable task. An attempt was made to compute these elements using an IBM 704 computer and a non-linear least squares program. (The programming for this problem was done by W. R. Busing of the Oak Ridge National Laboratory Chemistry Division.) Equations 19-21 were written in component form. "Best values" of the elements of A_α^2 and A_β^2 were sought such that $\sum [\Delta H_t(\text{observed})-\Delta H_t(\text{calc.})]^2$ would be a minimum. The details of this method will not be presented since it was not successful. It failed to yield sensible values of the tensor elements.

Fortunately, there were simplifying features of the spectra that allowed one of the tensors (A_α^2) to be determined directly in diagonal form. The resolved data of the ac plane show that, for one angle, the hyperfine interaction for the α nitrogen (N^{14}) is zero; as the field is rotated in this plane, the triplet structure characteristic of N^{14} collapses and only a doublet characteristic of N^{15} remains (see Figure 5a). From Equation 16 it is apparent that the only way this zero hyperfine splitting can occur is for a principal value of A_α^2 to be zero and for the magnetic field to be applied along the corresponding principal axis. A zero principal value is fortuitous as will be discussed in the next chapter when the detailed form of the hyperfine tensor is considered. If we assume that A_α^2 has but one zero principal value, it would seem even more coincidental that the corresponding principal axis should lie in the ac plane. This suggested that the A_α^2 tensor is axially symmetric and that an entire plane of zero splitting orientations should occur with this crystal. The strong doublet is indicative of the zero N^{14} splitting. A search for this doublet was carried out by orienting the crystal so that the magnetic field could be rotated in known crystallographic planes. Three planes, in addition to the ac plane, were searched (the 100, 001 and 011 planes). In planes other than the ac plane, this doublet would tend to be obscured by the lines from the "second" DPPH molecule. Because of the anomalous intensity behavior of the two DPPH molecules, sufficiently good resolution was obtained by confining the observations to the strong family of lines. In each of these planes, an orientation was found where a

strong doublet was seen superimposed on a spectrum of weaker lines. (See e.g. Figures 7c and 8c). The four orientations (including that found in the ac plane) defined a plane and confirmed axial symmetry. Three of the four orientations were coplanar to ca. $\pm 1^{\circ}$, the fourth deviated from this plane by about 5°. The direction normal to this plane is the unique axis of the axially symmetric tensor. It was found to make angles of 126°, 62°, and 36° respectively with the a, b, and c crystallographic axes. From this axis direction and from the elements of A_{α}^{2} obtained from the resolved data of the ac plane the only non-zero element of A_{α}^{2} was found to be 350.

The elements of A_{β}^{2} could then be deduced in a more conventional manner. Values of ΔH_{α} were calculated from the elements of A_{α}^{2} using Equation 20. Values of ΔH_{β} were then deduced using Equation 19 and from these the elements of A_{β}^{2} were computed. It was found that A_{β}^{2} would satisfactorily fit the data if it was also assumed to be axially symmetric. The tensor elements are presented in Table II. The elements of A_{α}^{2} and A_{β}^{2} are presented with reference to the axis system of Figure 13. The magnitudes of the principal values of A_{α} and A_{β} are also given. As indicated by Equation 18, only their magnitudes are determined experimentally. The directions of the unique principal axes of A_{α} and A_{β} are also shown in Table II. The angle between these axes was found to be 13° with an estimated uncertainty of $\pm 2^{\circ}$.

It is difficult to estimate the precision with which the tensor elements and the principle axes directions are known. Spectra calculated from the values listed above agree well with the measured data; generally

TABLE II

HYPERFINE TENSORS DEDUCED FROM PARAMAGNETIC RESONANCE SPECTRA OF LABELLED DPPH

Elements of A_α^2 and A_β^2 with Respect to Axis System of Figure 13

$$A_\alpha^2 = \begin{bmatrix} 38 & -55 & -94.5 \\ -55 & 79 & 135 \\ -94.5 & 135 & 233 \end{bmatrix} \qquad A_\beta^2 = \begin{bmatrix} 100 & -70 & -200 \\ -70 & 254 & 472 \\ -200 & 472 & 1260 \end{bmatrix}$$

Principal Values of A_α and A_β

$$A_\alpha = \begin{bmatrix} 0 & & \\ & 0 & \\ & & \pm 18.7 \end{bmatrix} \qquad A_\beta = \begin{bmatrix} \pm 8.2 & & \\ & \pm 8.2 & \\ & & \pm 38.5 \end{bmatrix}$$

Direction of Symmetry Axes for A_α and A_β

	Crystallographic Axes		
	a	b	c
A_α	126.5°	61.7°	36.3°
A_β	118.0°	68.7°	23.4°

the agreement is within one gauss. This comparison is shown graphically in Figures 9-11. Small deviations from axial symmetry might be expected to fit the data equally well. For example, the zero elements of A_α represent hyperfine components merging to a true singlet. This is illustrated in Figure 5 by a pair of triplets collapsing to a pair of singlets. Because of the natural width of the lines (ca. 7 gauss), a small spacing between the components of the triplet would not be resolved. However, the width and height of the pair of singlets (Figure 5) is very close to that predicted from the exact merging of the three hyperfine lines of 7 gauss half-width. This indicates that the small elements of A_α could not exceed one or two gauss. Similar uncertainties exist in A_β, since its evaluation was based in part on incompletely resolved data of the ab and bc planes, and since it depends upon the previous evaluation of the elements of A_α.

CHAPTER IV

INTERPRETATION AND DISCUSSION

In Chapter III, the paramagnetic resonance spectra of DPPH magnetically diluted in $DPPH_2$ were considered with reference to a spin Hamiltonian. The g-values were found to be essentially isotropic and very near the spin-only value, indicating that the orbital magnetism of the unpaired electron was almost completely quenched. Hyperfine spectra were found to be due to the hydrazyl nitrogens and, from these spectra, two tensors A_α and A_β were deduced. In this chapter the detailed form of these tensors is considered and some of the properties of the wave function for the unpaired electron are deduced.

Each of the hyperfine interactions terms of the Hamiltonian (Equation 4) has the detailed form[37]

$$\vec{S}\cdot A\cdot\vec{I} = \left[\frac{8\pi}{3}\,\Psi^2(0)\,\vec{S} - \left\langle\frac{\vec{S}}{r^3} - \frac{3\,\vec{S}\cdot\vec{r}\,\vec{r}}{r^5}\right\rangle\right]\cdot g_n\beta_n\vec{I} \qquad (23)$$

where $\vec{r}$ is a vector from the nucleus to the unpaired electron, r is its magnitude, $\Psi^2(0)$ is the unpaired electron density at r = 0, g_n is the nuclear g-value, and β_n is the nuclear magneton. These latter two quantities are defined in terms of the nuclear magnetic moment μ_n by the expression $g_n\beta_n = \mu_n/I$. The values $\beta_n = 5.049 \times 10^{-24}$ erg/gauss, $g_n(N^{14}) = 0.4036$, and $g_n(N^{15}) = -0.5660$ were used for this investigation (see e.g., Kopferman[39] for original sources). The angular brackets indicate averaging over the spatial parts of the wave function. It follows from Equation 23 that the elements of the hyperfine tensors are given by

$$A_{ij} = g_n\beta_n\left[\frac{8\pi}{3}\,\Psi^2(0)\,\delta_{ij} - \left\langle \frac{1}{r^3}\,(\delta_{ij} - 3x_ix_j/r^2)\right\rangle\right] \qquad (24)$$

In this equation, δ_{ij} is the Kronecker delta and the x_i are the components of $\vec{r}$ with respect to a suitable coordinate system. In diagonal form, using a matrix representation, Equation 24 becomes

$$A = g_n\beta_n\,\frac{8\pi}{3}\,\Psi^2(0)\begin{bmatrix}1 & & \\ & 1 & \\ & & 1\end{bmatrix} - g_n\beta_n\left\langle \frac{1}{r^3}\begin{bmatrix}1-3x_1^2/r^2 & & \\ & 1-3x_2^2/r^2 & \\ & & 1-3x_3^2/r^2\end{bmatrix}\right\rangle \qquad (25)$$

where x_1, x_2, and x_3 are the components of $\vec{r}$ with respect to the principal axes of the tensor. The first term C is the so-called contact term due to Fermi;[40] it arises from a relativistic treatment of the electron. The second term D, the dipolar term, represents the "classical" magnetic interaction of the electron spin dipole and the nuclear dipole. From Equation 25 we see that the experimental hyperfine tensors A_α and A_β can be resolved into two parts, C and D. The resolution is unique, since the elements of C are all the same ($C_1 = C_2 = C_3 = c$) and the trace of the dipolar part is zero ($D_1 + D_2 + D_3 = 0$).

Unfortunately, as was pointed out in the previous chapter, the signs of the elements of A_α and A_β could not be determined experimentally. Consequently, there were ambiguities in the resolution of the experimental tensors. The A_α tensor, because of the zero elements, gave least ambiguity:

$$\overset{A_\alpha}{\begin{bmatrix}0 & & \\ & 0 & \\ & & 18.7\end{bmatrix}} = \overset{C_\alpha}{\begin{bmatrix}6.3 & & \\ & 6.3 & \\ & & 6.3\end{bmatrix}} + \overset{D_\alpha}{\begin{bmatrix}-6.3 & & \\ & -6.3 & \\ & & 12.5\end{bmatrix}} \qquad (26)$$

A similar expression in which the sign of every element of each tensor is reversed is also possible. It was pointed out in Chapter III that

zero values for two of the principal elements of A_α were "fortuitous", and would not be expected in general. This can be seen with reference to Equation 26. Two of the elements of the contact tensor must be equal in magnitude, but opposite in sign to two of the elements of the dipolar tensor. The contact tensor is a measure of the s character of the unpaired electron distribution and the dipolar tensor is a measure of the p character. Thus, the amounts of s and p character of the unpaired electron distribution must balance appropriately if the two elements are to have the value zero.

Six resolutions of A_β are possible depending on the signs of the elements. Three of these are: (for purposes of comparison, the elements of A_β, deduced for N^{15}, have been converted to values appropriate to N^{14} by multiplying each element by $g_{14}/g_{15} = -0.7129$).

$$\overset{A_\beta}{\begin{bmatrix} 5.8 & & \\ & 5.8 & \\ & & 27.5 \end{bmatrix}} = \overset{C_\beta}{\begin{bmatrix} 13.0 & & \\ & 13.0 & \\ & & 13.0 \end{bmatrix}} + \overset{D_\beta}{\begin{bmatrix} -7.2 & & \\ & -7.2 & \\ & & 14.5 \end{bmatrix}} \quad (27)$$

$$\begin{bmatrix} -5.8 & & \\ & -5.8 & \\ & & 27.5 \end{bmatrix} = \begin{bmatrix} 5.3 & & \\ & 5.3 & \\ & & 5.3 \end{bmatrix} + \begin{bmatrix} -11.1 & & \\ & -11.1 & \\ & & 22.2 \end{bmatrix} \quad (28)$$

$$\begin{bmatrix} 5.8 & & \\ & -5.8 & \\ & & 27.5 \end{bmatrix} = \begin{bmatrix} 9.1 & & \\ & 9.1 & \\ & & 9.1 \end{bmatrix} + \begin{bmatrix} -3.3 & & \\ & -14.9 & \\ & & 18.3 \end{bmatrix} \quad (29)$$

The other three resolutions are similar, but with the sign of every element reversed.

The resolutions of A_α and A_β presented in Equations 26-29 are the only ones which may be interpreted in terms of a wave function for a single unpaired electron. If the resolutions of opposite sign were chosen, such an interpretation would not be possible. For example, the elements of the contact tensors are defined by Equation 25 to be $c = 8\pi g_n \beta_n \Psi^2(0)/3$. Only positive quantities enter this expression (g_n refers to N^{14} and is positive), hence resolutions yielding negative values of c_α or c_β need not be considered in this one electron treatment.*

The hyperfine interaction is predominantly sensitive to the unpaired electron distribution in the vicinity of a magnetic nucleus; the contact coupling depends on $\Psi^2(0)$, and the dipolar term involves $1/r^3$. The tensors deduced from the experimental data thus relate only to that part of the wave function of the unpaired electron in the neighborhood of the hydrazyl nitrogens. It is reasonable to assume that the wave function in the vicinity of the hydrazyl nitrogen nuclei can be represented as a linear combination of atomic orbitals, Ψ_α and Ψ_β, centered on these nuclei;

$$\Psi = a_\alpha \Psi_\alpha + a_\beta \Psi_\beta, \tag{30}$$

and that Ψ_α and Ψ_β are nitrogen 2s-2p hybrids;

---

*This simple one electron description is only approximate, but adequately describes the features of the electronic structure of DPPH that can be ascertained from the experimental data. In a more complete description, both positive and negative values of A_α are permitted. The concept of spin density[41,42] rather than electron density is used to interpret the hyperfine interactions. The consequences of this refinement will be considered later in more detail.

$$a_\alpha \Psi_\alpha = a_{s\alpha}\, \Psi_{s\alpha} + a_{p\alpha}\, \Psi_{p\alpha} \tag{31}$$

$$a_\beta \Psi_\beta = a_{s\beta}\, \Psi_{s\beta} + a_{p\beta}\, \Psi_{p\beta} \ . \tag{32}$$

Only the s orbitals contribute to the contact tensor, i.e. $\Psi^2(0) = a_s^2\ \Psi_s^2(0)$. Thus, from Equation 25, the s electron density about a given nucleus is

$$a_s^2 = \frac{3c}{8\pi g_n \beta_n\ \Psi_s^2(0)} \ . \tag{33}$$

In this equation c is an element of an experimental contact tensor (Equations 26-29).

The angular brackets of Equation 25 indicate an averaging with respect to the wave function Ψ. The elements of D_α are given by

$$(D_\alpha)_i = g_n \beta_n \int \Psi^2 \left[\frac{1}{r^3}\,(1-3x_i^2/r^2)\right]_\alpha d\tau \ . \tag{34}$$

The subscript α indicates that r and x_i are measured with respect to the α nitrogen nucleus. A similar equation, of course, relates the elements of D_β. In the development which follows, only expressions relating to the α nitrogen will be given. The equations for the β nitrogen may be obtained by interchanging the α and β indices. If we expand Ψ^2 using Equation 30, three terms result:

$$\begin{aligned}(D_\alpha)_i = -g_n\beta_n \Big\{ & a_\alpha^2 \int \Psi_\alpha^2 \left[\frac{1}{r^3}\,(1 - 3x_i^2/r^2)\right]_\alpha d\tau \\ & + a_\beta^2 \int \Psi_\beta^2 \left[\frac{1}{r^3}\,(1 - 3x_i^2/r^2)\right]_\alpha d\tau \\ & + 2a_\alpha a_\beta \int \Psi_\alpha \Psi_\beta \left[\frac{1}{r^3}\,(1 - 3x_i^2/r^2)\right]_\alpha d\tau . \end{aligned} \tag{35}$$

The first term of Equation 35 represents the magnetic dipole interaction of the electron with the α nitrogen nucleus when the electron is considered to be in orbitals centered on this nucleus. The second term represents

this interaction when the electron is in orbitals centered on the β nitrogen. The third represents the interaction from the overlap region. Because of the $1/r^3$ dependence, the value of the first term is large compared to the others. The others may be neglected since the values are within the limits of experimental error. This point is considered in more detail after the first term is evaluated.

On expanding Ψ_α^2 by Equation 31, three terms are obtained:

$$(D_\alpha)_i \approx -g_n\beta_n\left\{a_{p\alpha}^2 \int \Psi_{p\alpha}^2\left[\frac{1}{r^3}\,(1 - 3x_i^2/r^2)\right]_\alpha d\tau + a_{s\alpha}^2 \int \Psi_{s\alpha}^2\left[\frac{1}{r^3}\,(1 - 3x_i^2/r^2)\right]_\alpha d\tau + 2a_{s\alpha}\, a_{p\alpha} \int \Psi_{s\alpha}\Psi_{p\alpha}\left[\frac{1}{r^3}\,(1 - 3x_i^2/r^2)\right]_\alpha d\tau\right\}. \quad (36)$$

An approximate equality is indicated because of the exclusion of the second and third terms of Equation 35. The last two terms of Equation 36 are equal to zero as can be seen by integrating the angularly dependent terms. The elements of D_α depend only on the p-orbital centered on the α nitrogen. A quenched p-orbital may be described by $\Psi_p = f(r)z$, where z is the symmetry axis of the p orbital and f(r) specifies the radial dependence of the function. Using this function and carrying out the appropriate integrations of Equation 36, it is found that

$$D_\alpha \approx \frac{2}{5}\, g_n\beta_n\, a_{p\alpha}^2 \left\langle \frac{1}{r_\alpha^3} \right\rangle_p \begin{bmatrix} -1 & & \\ & -1 & \\ & & 2 \end{bmatrix} . \quad (37)$$

The evaluation of $\langle 1/r_\alpha^3 \rangle_p$ depends on the detailed form of the radial part of the wave function.

A model of the unpaired electron distribution must be assumed in order to evaluate the contribution to D_α from the second term of Equation 35. It was assumed that the unpaired electron distribution is adequately

described by Slater 2p orbitals, one centered on each nitrogen; that these orbitals are parallel to each other and perpendicular to the N-N bond direction; and that the N-N distance is 1.45 Å (that of hydrazine). The term as written in Equation 35 was not used. Trammell, Zeldes, and Livingston[38] have considered this interaction in a somewhat different form and have developed equations (Equations 15 and 19 of reference 38) from which the interaction can be readily evaluated. It was found that the contribution to D_α from the second term of Equation 35 is

$$a^2_{p\beta} \begin{bmatrix} -0.40 & & \\ & 0.65 & \\ & & -0.25 \end{bmatrix} .$$

Even with the extreme assumption that $a^2_{p\beta} = 1$, the elements given above are small compared to the elements of D_α in Equations 26-29 and are within the limits to which they are known experimentally. The third term of Equation 35 contributes even less to D_α. Contributions from this term depend on the overlap of the two p orbitals. Assuming again an N-N distance of 1.45 Å, overlap will be very small and the $1/r^3$ dependence will reduce the contribution even more. Consequently, the contribution from both of these terms may be neglected.

The dipolar tensor of Equation 37 and the experimentally observed dipolar tensors (excepting that of Equation 29 which will be discussed below) are axially symmetric. Their elements may be equated and solved for a^2_p:

$$a^2_p = \frac{D_3}{4/5\ g_n\beta_n \langle 1/r^3 \rangle p} . \qquad (38)$$

Here, D_3 is the unique element of the observed dipolar tensors.

We have seen that the electron distribution in the vicinity of the β nitrogen (Ψ_β) contributes predominantly to D_β, and if this distribution is assumed to be an s-p hybrid D_β will be very nearly axially symmetric. The distinctly non-axially symmetric tensor D_β obtained from one resolution of A_β (Equation 29) is therefore physically unacceptable. That this resolution is unacceptable is further supported by the unique resolution of A_α into an axially symmetric dipolar tensor; it would seem highly unlikely that the electronic distributions about the two nitrogens should differ so much.

To apply Equations 25 and 38 to the experimental tensors, values for $\Psi_s^2(0)$ and $\langle 1/r^3 \rangle_p$ are needed. Hartree-Fock[43] wave functions for a nitrogen 2s electron were used to evaluate $\Psi_s^2(0)$. A value of 32.0 x 10^{24} cm.$^{-3}$ was found. A value of $\langle 1/r^3 \rangle_p$ = 20.8 x 10^{24} cm.$^{-3}$ was found using nitrogen 2p functions (^{4}S state). Dousmanis[44] points out that the Hartree-Fock functions will underestimate this value and recommends $\langle 1/r^3 \rangle_p$ = 22.5 x 10^{24} cm.$^{-3}$. This value was used to evaluate $a_{p\beta}^2$. To evaluate $a_{p\alpha}^2$ the following resonant structures of DPPH have been considered:

(a) (b)

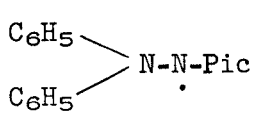

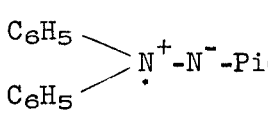

(39)

When the unpaired electron is regarded as being on the α nitrogen, this nitrogen has a positive formal charge. The 2p electron is more tightly bound; it is screened somewhat less from the nuclear charge and an increase in $\langle 1/r^3 \rangle_p$ is expected. Hartree functions for N^+ are not available. Townes and Schawlow[45] have considered the effect of nuclear charge and have found

that $\langle 1/r^3 \rangle_p$ must be increased by a factor of 1.30 to account for the decrease in screening. Thus, the value $\langle 1/r^3 \rangle_p = 29.2 \times 10^{24}$ cm.$^{-3}$ was used for the α nitrogen. An increase in $\Psi_s^2(0)$ for the α nitrogen would likewise be expected, but since no reliable method for estimating the increase is known and since a_s^2 values were found to be small on both nitrogens, the same value was used for both nitrogens. On inserting the appropriate numerical parameters into Equations 33 and 38, the following equations relating to the s and p character of the electron distribution were obtained:

$$a_s^2 = c/546 \tag{40}$$

$$a_{p\alpha}^2 = D_{\alpha 3}/47.7 \tag{41}$$

$$a_{p\beta}^2 = D_{\beta 3}/36.7 \ . \tag{42}$$

Using the above equations, the following results were obtained. For α nitrogen

$$a_{s\alpha}^2 = 0.011 \text{ and } a_{p\alpha}^2 = 0.263 \ . \tag{43}$$

The total unpaired electron density is 0.274 of which 4 per cent is s character. For the β nitrogen there are two choices depending on the resolution used. For the resolution of Equation 27

$$a_{s\beta}^2 = 0.024 \text{ and } a_{p\beta}^2 = 0.396 \ . \tag{44}$$

The total electron density is 0.420 of which 5.7 per cent is s character. For the resolution of Equation 28

$$a_{s\beta}^2 = 0.010 \text{ and } a_{p\beta}^2 = 0.605 \ . \tag{45}$$

The total electron density is 0.615 of which 1.6 per cent is s character.

Weissman[46] has shown that only the contact terms in the hyperfine interaction contribute to hyperfine spectra observed in solution. It was

hoped that a comparison of the contact coupling constants c_α and c_β deduced from the DPPH-$DPPH_2$ crystals (Equations 26-28) with those deduced from DPPH solutions would remove the ambiguity in the resolution of A_β. Deal and Koski[25] have investigated the detailed shape of the paramagnetic resonance spectrum of DPPH in solution and found that the ratio of the contact coupling coefficients was 0.82 ± 0.01. Since their analysis was carried out with normal DPPH, they were unable to determine whether c_α or c_β was larger. A similar analysis has been carried out recently by Weil[47] and co-workers using both normal and labelled (N^{15} in the β nitrogen position) DPPH. This analysis established that, in solution, $c_\alpha < c_\beta$. The ratio found $c_\alpha/c_\beta = 0.77$ is in essential agreement with that of Koski. This result is not in agreement with the results found in this work on DPPH in a single crystal. A ratio $c_\alpha/c_\beta = 0.48$ is indicated if the resolutions of Equations 26 and 27 are preferred and a ratio $c_\alpha/c_\beta = 1.19$ is indicated using Equations 26 and 28.

We have seen from Equations 43-45 that the contact interaction, the only part observed in solution, represents a minor portion of the electron density ($a^2_{s\alpha} = 0.011$; $a^2_{s\beta} = 0.024$ or 0.010). Presumably, this small amount of s admixture might vary with the environment of the DPPH molecule, and cause corresponding changes in the hyperfine spectra. The overall splitting ΔH_t of the normal DPPH solution spectrum is a measure of the sum of the contact coupling coefficients. This splitting was measured under a variety of conditions to see if it was sensitive to environmental effects. Measurements were made in benzene solution (0.002 and 0.005 M DPPH) and in carbon disulfide solution (0.005 M).

The measurements were repeated with the solutions saturated with $DPPH_2$. The spectra were essentially the same in all cases. All measurements of ΔH_t were found to fall within one gauss of 34 gauss. While the uncertainty quoted may possibly be due to small environmental effects, it is within the estimated accuracy of the measurements. The DPPH molecule in the $DPPH_2$ lattice is undoubtedly somewhat distorted from its structure in solution and relatively large differences in contact hyperfine couplings might occur. A study of DPPH in different host crystals should help to elucidate this environmental effect. As noted in Chapter II, several attempts were made to grow such crystals without success.

Thus, the solution results are not definative in removing the ambiguity in the possible resolution of A_β. With either choice of resolution, however, the unpaired electron density on the β nitrogen is greater than that on the α nitrogen, indicating that the resonant structure (a) of Equation 39 predominates. This is the structure a chemist would normally write for DPPH. The electron densities determined here are substantially different from those calculated by a molecular orbital method[48] which give unpaired electron densities of 0.1416 and 0.1518 respectively for the α and β nitrogens. The unpaired electron was found in this investigation to be predominantly in p orbitals. The symmetry axes of these orbitals were found to make an angle of 13° with each other. It is reasonable to assume that these orbitals are approximately perpendicular to the N-N bond. This cannot be stated with certainty, however, since the orientation of the DPPH molecule with respect to the crystal axes is not known.

For a free radical such as DPPH the total spin S^2 and its component in the field direction S_z are conserved; i.e. in a magnetic field, in the lowest energy state, $S^2 = \frac{1}{2}(\frac{1}{2} + 1)$ and $S_z = \frac{1}{2}$. The spins of the individual electrons contribute to S_z ($S_z = \sum_i s_{zi}$). Most of the electrons are paired in bonding orbitals or inner shells and do not contribute to S_z. In describing the paramagnetic resonance spectra of DPPH, we have assumed that all of the electrons but one are paired and have found that this approximation is adequate to describe the experimental data. It has been shown[41,42,49] both theoretically and experimentally, however, that this simple description may not be generally adequate. We shall examine at this time some of the consequences of a more complete description. In a free radical, configurations involving more than one unpaired electron may be important. For example, a configuration in which $S_z = 1/2$ might involve three electrons in different orbitals, two with $s_z = 1/2$ and the third with $s_z = -1/2$. Each of the unpaired electrons, however, produces a magnetic field at the nuclear position and each must be considered in interpreting the hyperfine splittings. For this purpose, a spin density function[41,42] has been defined:

$$\rho(x,y,z) = 1/S_z \left\langle \sum_i s_{zi} \delta(r_i) \right\rangle . \qquad (46)$$

The angular brackets indicate an expectation over the complete wave function of the molecule and $\delta(r_i)$ is the Dirac delta function of the distance between the electron i and the point x,y,z in space. The density of spin angular momentum (spin density) at the point x,y,z is expressed by ρS_z; thus ρ is a normalized spin density. When the total wave function is approximated by a one electron wave function the spin

density ρ and the electron density $\Psi^2(x,y,z)$ are identical. In a real molecule, however, the spin density at a given point may be either positive or negative. The integral of ρ over all space is unity; this statement defines the conservation of total spin S_z.

The equations developed in Chapter III to describe the observed hyperfine splittings are not altered by these considerations. The hyperfine tensors A_α and A_β must be interpreted in a somewhat different light however. The contact and dipolar tensors respectively are given by equations completely analogous to Equations 33 and 38 but in which the electron density Ψ^2 is replaced by the spin density ρ. Thus, the tensor elements c and D_3 may be either positive or negative; i.e. in addition to the resolutions of A_α and A_β given by Equations 26, 27, and 28 we must consider other resolutions in which the signs of every element in these equations are reversed. Negative values of c_α, for example, would require negative spin densities at the position of the α nitrogen nucleus, and would signify that those configurations in which the spin part of the s function was antiparallel to the total spin were predominant. Similarly, a negative value of $D_{3\alpha}$ would signify that the spin density integrated over the p orbital centered on the α nitrogen was negative.

The values of a_s^2 and a_p^2 calculated earlier refer to the absolute magnitude of the integrated spin density. Since the sign of c and the sign of D_3 in both of Equations 26 and 28 are the same, the spin associated with the s orbital and the spin associated with the p orbital are of the same sign on each nitrogen. The total integrated spin densities, the sum of the s and p contributions, are $a_\alpha^2 = \pm 0.274$ and $a_\beta^2 = \pm 0.420$ or

± 0.615. There were no experimental indications of the sign of these quantities. The choice with each quantity positive is favored, however. In this case the total spin associated with the hydrazyl nitrogens is 0.694 or 0.889 and indicates that the electron spin is highly localized on these nitrogens. The only other reasonable choice is with $+ a_{\beta}^{2}$ and $- a_{\alpha}^{2}$. This choice would correspond to a total spin of 0.146 or 0.341 on the hydrazyl nitrogens and, by difference, a large amount of spin would be on the phenyl and picryl rings.

Resolved hyperfine splittings from the hydrogen and nitrogen nuclei of the aromatic rings were not seen. Indeed, the width of the individual lines (ca. 7 gauss) is typical of hydrogenous materials and indicates that hyperfine interactions with the ring nuclei are weak. A recent nuclear magnetic resonance study[50] of the shift of the proton resonances of DPPH indicates that hyperfine splittings from the aromatic hydrogens should be about 1 gauss. Splittings this small would, of course, be unresolved in the experiments reported here. The NMR proton resonance shifts have been related to electron spin densities on the aromatic carbons; spin densities of ca. 0.07 on the ortho and para phenyl carbons and ca. - 0.04 on the meta carbons of both phenyls and the picryl group were indicated. These values appear to be in much better accord with the assumption of positive spin densities on both hydrazyl nitrogens.

BIBLIOGRAPHY

1. E. Zavoisky, J. Phys. U. S. S. R., 9, 211 (1945).

2. B. Bleaney and K. W. H. Stevens, Repts. Progr. in Phys., 16, 108 (1953).

3. K. D. Bowers and J. Owen, Repts. Progr. in Phys., 18, 304 (1955).

4. D. M. S. Bagguley and J. Owen, Repts. Progr. in Phys., 20, 304 (1957).

5. J. W. Orton, Repts. Progr. in Phys., 22, 204 (1959).

6. J. E. Wertz, Chem. Rev., 55, 829 (1955).

7. D. J. E. Ingram, "Free Radicals as Studied by Electron Spin Resonance," Butterworth Scientific Publications, London, 1958.

8. L. Pauling and S. Goudsmit, "The Structure of Line Spectra," McGraw Hill Book Co., Inc., New York, 1930.

9. S. Weissman, Z. Electrochem., 64, 47 (1960).

10. S. Goldschmidt and K. Renn, Ber., 55, 628 (1922).

11. J. Turkevich and P. W. Selwood, J. Am. Chem. Soc., 63, 1077 (1941).

12. P. W. Selwood, "Magnetochemistry," 2nd ed., Interscience Publishers, Inc., New York, 1956, p. 266.

13. A. N. Holden, C. Kittel, F. R. Merritt, and W. A. Yager, Phys. Rev., 77, 147 (1950).

14. C. H. Townes and J. Turkevitch, Phys. Rev. 77, 148 (1950).

15. C. A. Hutchison, Jr., R. C. Pastor, and A. G. Kowalski, J. Chem.Phys., 20, 534 (1952).

16. G. Berthet, Compt. rend., 240, 57 (1955).

17. R. Livingston and H. Zeldes, J. Chem. Phys., 24, 170 (1956).

18. A. van Roggen and W. Gordy, Phys. Rev., 105, 50 (1957).

19. L. S. Singer and C. Kikuchi, J. Chem. Phys., 23, 1738 (1955).

20. J. Herve, Compt. rend., 245, 653 (1957).

21. J. Lothe and G. Eia, Acta Chem. Scand., 12, 1535 (1958).

22. H. S. Jarrett, J. Chem. Phys., 21, 761 (1953).

23. J. Herve, Compt. rend., 246, 262 (1958).

24. G. E. Pake and T. R. Tuttle, Jr., Phys. Rev. Letters, 3, 423 (1959).

25. R. M. Deal and W. S. Koski, J. Chem. Phys., 31, 1138 (1959).

26. C. Kikuchi and V. W. Cohen, Phys. Rev., 93, 394 (1954).

27. Y. Deguchi, J. Chem. Phys., 32, 1584 (1960).

28. K. J. Mysels, J. Chem. Ed., 36, 303 (1959).

29. D. F. Heath, J. Chem. Soc., 4152 (1957).

30. A. Murray and D. L. Williams, "Organic Syntheses with Isotopes," Interscience Publishers, Inc., New York, 1958, p. 1830.

31. K. Clusius and M. Vecchi, Helv. Chim. Acta, 36, 933 (1953).

32. R. H. Porier, E. J. Kahler, and F. Benington, J. Org. Chem., 7, 1435 (1952).

33. M. Sternberg, Compt. rend., 240, 990 (1955).

34. R. D. Ellison and R. W. Holmberg, Acta Cryst., 13, 446 (1960).

35. E. L. Gintzon, "Microwave Measurements," McGraw Hill Book Co., Inc., New York, 1957.

36. H. A. Thomas, R. L. Driscoll, and J. A. Hipple, Phys. Rev., 78, 787 (1950).

37. A. Abragam and M. H. L. Pryce, Proc. Roy. Soc. (London) A205, 135 (1951).

38. G. T. Trammell, H. Zeldes, and R. Livingston, Phys. Rev., 110, 630 (1958).

H. Zeldes, G. T. Trammell, R. Livingston, and R. W. Holmberg, J. Chem. Phys., 32, 618 (1960).

39. H. Kopferman, "Nuclear Moments," Academic Press, Inc., New York, 1958.

40. E. Fermi, Z. Physik., 60, 320 (1930).

41. H. A. McConnell and D. B. Chesnut, J. Chem. Phys., 28, 107 (1958).

42. F. C. Adams and S. Weissman, J. Am. Chem. Soc., 80, 2057 (1958).

43. D. R. Hartree and W. Hartree, Proc. Roy. Soc. (London) A193, 299 (1948).

44. G. C. Dousmanis, Phys. Rev., 97, 967 (1955).

45. C. H. Townes and A. L. Schawlow, "Microwave Spectroscopy," McGraw Hill Book Company, Inc., New York, 1955, p. 239.

46. S. I. Weissman, J. Chem. Phys., 22, 1378 (1954).

47. Private communication from John Weil, Argonne National Laboratory, September 20, 1960.

48. R. Bersohn, Arch. Sci. (Geneva) 11, 12 (1958).

49. H. M. McConnell, J. Chem. Phys., 28, 1188 (1958).

50. H. S. Gutowsky, H. Kusumoto, T. H. Brown, and D. H. Anderson, J. Chem. Phys., 30, 860 (1959).

ORNL-3052
UC-4 - Chemistry-General
TID-4500 (15th ed.)

INTERNAL DISTRIBUTION

1. C. E. Center
2. Biology Library
3. Health Physics Library
4-5. Central Research Library
6. Reactor Division Library
7-26. Laboratory Records Department
27. Laboratory Records, ORNL R.C.
28. A. M. Weinberg
29. L. B. Emlet (K-25)
30. J. P. Murray (Y-12)
31. J. A. Swartout
32. E. H. Taylor
33. E. D. Shipley
34. S. C. Lind
35. M. L. Nelson
36. C. P. Keim
37. J. H. Frye, Jr.
38. R. S. Livingston
39. F. L. Culler
40. A. H. Snell
41. A. Hollaender
42. M. T. Kelley
43. K. Z. Morgan
44-53. R. W. Holmberg
54. J. W. Youngblood
55. T. A. Lincoln
56. A. S. Householder
57. C. S. Harrill
58. C. E. Winters
59. H. E. Seagren
60. D. Phillips
61. D. S. Billington
62. J. A. Lane
63. M. J. Skinner
64. W. H. Jordan
65. G. E. Boyd
66. R. A. Charpie
67. R. S. Cockreham
68. P. M. Reyling
69. Bryce Crawford (consultant)
70. T. H. Davies (consultant)
71. L. D. Roberts (consultant)
72. G. T. Seaborg (consultant)
73. C. E. Larson (consultant)
74. ORNL - Y-12 Technical Library, Document Reference Section

EXTERNAL DISTRIBUTION

75. Division of Research and Development, AEC, ORO
76-557. Given distribution as shown in TID-4500 (15th ed.) under Chemistry-General category